Shape Optimization of Polynomial Functionals under Uncertainties on the Right-Hand Side of the State Equation

Fabien Caubet, Marc Dambrine, Giulio Gargantini, Jérôme Maynadier

Shape Optimization of Polynomial Functionals under Uncertainties on the Right-Hand Side of the State Equation

Fabien Caubet[1], Marc Dambrine[1], Giulio Gargantini[1,2] and Jérôme Maynadier[2]

[1]E2S UPPA, CNRS, LMAP, UMR 5142, Université de Pau et de Pays de l'Adour, Pau, 64000, France.
[2]Safran Helicopter Engines, Avenue Joseph Szydlowski, Bordes, 64510, France.

Corresponding authors. E-mails: fabien.caubet@univ-pau.fr; marc.dambrine@univ-pau.fr; giulio.gargantini@univ-pau.fr; jerome.maynadier@safrangroup.com;

Abstract

The present paper is dedicated to a problem of shape optimization where the external loads applied to the structure are subject to uncertainties. The objective functional or the constraints can be written as the expected value of a polynomial functional of degree $\boldsymbol{m}$. We provide a deterministic expression of the expectation of the polynomial as a function of the first $\boldsymbol{m}$ moments of the random variables modeling the uncertainties, as well as a method to compute its shape derivative according to Hadamard. In particular, no further assumptions on the distribution of the random variables are required, and the method presented in this article is not based on computationally expensive sampling techniques. The proposed method can be applied in different contexts, like the study of the variance of a quadratic functional, or the optimization of a functional approaching the $\mathbf{L}^{\boldsymbol{\infty}}$-norm of a quantity in the structure.

Keywords: Shape optimization, random right-hand side, linear elasticity, von Mises stress, polynomial functional.

MSC Classification: 49Q10 , 65N75 , 65C20 , 65K10.

Contents

1 Introduction

Shape and topology optimization are topics of ever increasing interest in the domains of engineering. The design of mechanical structures satisfying several constraints of different natures is a difficult problem for engineers, and shape optimization techniques offer an automated approach to devise original designs which are compliant with the given constraints. In the context of mechanical engineering, the optimization problem often concerns the optimization of elastic structures satisfying some requirements on their mass, and their robustness under a given mechanical load. Such robustness is usually estimated using the mechanical compliance of the structure, or computing some yield criterion like the evaluation of the von Mises stress (see e.g. [1] and [2]).

The increasing demand of optimized structures and the progress in computational science have resulted in the development of different optimization

techniques. The approach considered in this paper relies on Hadamard's boundary variation method, treated extensively in [3], [4], and in chapter 5 of [5]. The profile of the structure is represented numerically using a level-set approach on conforming and non-conforming meshes (see [6] for a comprehensive review of the level-set method, and [7–10] for its application in the context of shape optimization). Other approaches to topology optimization include the class of density methods (see [11, 12]), among which the Solid Isotropic Material with Penalization (SIMP) method is the most widely encountered. We refer the reader to [13] and [12], and to the review paper [14] for further information on the several techniques of shape and topology optimization. As of today, the main design softwares available on the market offer tools for structure optimization, integrating new features and developments at each release of a new version.

In industrial applications it is unrealistic to consider that all information on the problem is perfectly known. On the contrary, the presence of uncertainties on the geometry, on the material properties, and on the external loads applied on the structure must be accounted for in the design in order to assure a correct manifacturing process and the performances of the device. The handling of uncertainties on the shape of the domain is studied in [15] and in [16]. In [17] the authors address the issue of small uncertainties on the material properties, on the external loads, and on the geometry of the structure by linearizing the perturbation around their mean value. In [18] the mean and the variance of a generic objective functional are estimated using a dimension reduction method followed by a Gauss-type quadrature sampling, while the shape sensitivities are computed using the analitical derivatives of the random moments. The authors of [19] study the minimization of the mean and the variance of the mechanical compliance of an elastic structure, considering an exact expression of the random moments and their sensitivities with respect to the shape. A similar approach is adopted in [20], where the authors provide a method to compute analytically the expected value of a generic quadratic functional in terms of the first and second moments of the random variables modeling the uncertainties.

The present work adapts and extends the approach of [20] to the case of polynomial functionals. We consider the shape optimization problem as an instance of a PDE-constrained optimization problem, where the solution is an element of a given Banach space. We suppose the right-hand side of the partial differential equation to be subject to uncertainties, without any assumption on their amplitude, and the uncertainties are modeled as random variables, using suitable Bochner spaces. Let m be the degree of the polynomial functional of interest. Similarly to the procedure detailed in [20], we introduce a deterministic correlation tensor of order m, which depends only on the first m random moments. By consequence, it is possible to compute exactly the expected value of the functional of interest, as well as its shape derivative in terms of the first m moments of the random variables modeling the uncertainties, without any further assumption on their distributions. Notably, no sampling method

requiring a large number of simulations is used in the method presented here. The procedure detailed in this paper allows for the optimization of a structure with respect to the variance of a quadratic functional (like the mechanical compliance), which can be expressed as a polynomial functional of degree 4. Another application is related to the utilization of the L^m-norm of a function as a smooth approximation of its L^∞-norm (i.e. its supremum) in a given domain. Indeed, by considering the L^m-norm of the stress in the domain as functional of interest , we are able to derive shapes where, on average, stress are less concentrated than in the ones obtained by controlling the expectation of the mechanical compliance.

This article is organized as follows. In section 2 we introduce the mathematical structures and techniques that are necessary for the statement of the shape optimization problem and for its solution. In particular, we recall the definition and properties of Hadamard's shape derivative, we present the notion of tensor product between Banach spaces and of projective product space, and we outline a model for the treatment of the uncertainties. Section 3 states the main results of this article, it introduces the correlation operator for multilinear functionals and its applications in the context of shape optimization, with a particular focus on the context of linear elasticity. Section 4 and section 5 provide two examples of numerical applications. In section 4 a tridimensional structure is subject to an uncertain load, and its mass is minimized under a constraint on the L^6-norm of the von Mises stress in the domain. Such example adresses the common concern in structural mechanics in avoiding the concentration of stress in a small region of the structure. Section 5 treats a bidimensional example, and shows how taking into account the variance of the compliance in a shape optimization problem can be crucial when the random variable modeling the mechanical loads are heavily correlated. Finally, the conclusions are drawn in section 6.

2 Mathematical setting and tools

2.1 Shape optimization

Let us consider a bounded domain $\Omega \subset \mathbb{R}^d$ with Lipschitz continuous boundary, for dimension $d = 2$ or 3. If $\boldsymbol{\theta} \in \mathrm{W}^{1,\infty}\left(\mathbb{R}^d, \mathbb{R}^d\right)$ is a Lipschitz continuous vector field such that $\|\boldsymbol{\theta}\|_{1,\infty} = \|\boldsymbol{\theta}\|_\infty + \|\nabla\boldsymbol{\theta}\|_\infty < 1$, we define the deformed domain $\Omega_{\boldsymbol{\theta}}$ as $\Omega_{\boldsymbol{\theta}} = (\mathbb{I} + \boldsymbol{\theta})\,\Omega$. For the sake of simplicity, we consider a class of admissible shapes $\mathcal{S}_{adm}$, and a class Θ_{adm} of vector fields such that, for all $\boldsymbol{\theta} \in \Theta_{adm}$, the deformed set $\Omega_{\boldsymbol{\theta}}$ belongs to $\mathcal{S}_{adm}$. Let $J(\cdot)$ be a shape functional $J : \mathcal{S}_{adm} \to \mathbb{R}$, that is supposed to be sufficiently regular. At first, we recall the notion of shape differentiability, as introduced in chapter 5 of [5] or in section 6.3 of [4].

Definition 2.1 (Fréchet differentiable shape functional) *A shape functional is* ***Fréchet differentiable*** *at Ω if there exists a linear continuous function $J'(\Omega)(\cdot)$:*

$\mathrm{W}^{1,\infty}\left(\mathbb{R}^d, \mathbb{R}^d\right) \to \mathbb{R}$ *such that*

$$J(\Omega_{\boldsymbol{\theta}}) = J(\Omega) + J'(\Omega)(\boldsymbol{\theta}) + o(\boldsymbol{\theta})$$

for all $\boldsymbol{\theta} \in \mathrm{W}^{1,\infty}\left(\mathbb{R}^d, \mathbb{R}^d\right)$, *where* $\lim_{\boldsymbol{\theta}\to 0} \frac{o(\boldsymbol{\theta})}{\|\boldsymbol{\theta}\|_{1,\infty}} = 0$. *The linear form* $J'(\Omega)(\cdot)$ *is called* ***shape derivative*** *of* J *in* Ω.

If the domain Ω is sufficiently regular, we can assume that the value of the derivative $J'(\Omega)(\boldsymbol{\theta})$ depends only on the normal component of the vector field $\boldsymbol{\theta}$ on the surface $\partial\Omega$ of the domain. Such result derives from the following *structure theorem*, proven by Hadamard and stated as Proposition 5.9.1 in [5]:

Theorem 2.1 (Hadamard's structure theorem) *Let* $\Omega \in \mathcal{S}_{adm}$ *be a* $\mathcal{C}^1$ *domain, and let us denote* $\mathbf{n}(\mathbf{x})$ *the vector normal to the surface* $\partial\Omega$ *in* $\mathbf{x} \in \partial\Omega$. *We suppose that* $J : \mathcal{S}_{adm} \to \mathbb{R}$ *is a differentiable functional. If* $(\boldsymbol{\theta} \cdot \mathbf{n}) = 0$ *on the entire surface* $\partial\Omega$, *then* $J'(\Omega)(\boldsymbol{\theta}) = 0$.

In the context of shape optimization, the shape derivative is used to identify a direction of deformation $\boldsymbol{\theta}_{\text{def}}$ such that $J'(\Omega)(\boldsymbol{\theta}_{\text{def}}) < 0$, which acts as direction of descent in a suitable gradient-based optimization algorithm (see e.g. [13, 21, 22]).

2.2 Tensor product in Banach spaces

In [20], the tensor product between Hilbert spaces is used to replace the quadratic objective functional with a linear one. The approach is extended to the case of functionals of degree $m > 2$ by considering the projective tensor product in Banach spaces, as defined in [23]. At first, we define the tensor product between multiple vector spaces.

Definition 2.2 (Tensor product between vector spaces) *For a positive integer* $m \geq 2$, *let us consider the vector spaces* $X_1, \ldots, X_m$. *We denote* $\hat{\mathfrak{P}}_m(X_1, \ldots, X_m)$ *the space of all m-multilinear forms on* $\prod_{i=1}^m X_i$. *For* $(x_1, \ldots, x_m) \in \prod_{i=1}^m X_i$, *the* ***tensor product*** $x_1 \otimes \ldots \otimes x_m$, *also written as* $\bigotimes_{i=1}^m x_i$, *is a real valued linear application defined on* $\hat{\mathfrak{P}}_m(X_1, \ldots, X_m)$ *such that, for all* $P_m \in \hat{\mathfrak{P}}_m(X_1, \ldots, X_m)$,

$$\left(\bigotimes_{i=1}^m x_i\right)(P_m) = P_m(x_1, \ldots, x_m).$$

The tensor product of the vector spaces $X_1, \ldots, X_m$ *is defined as:*

$$\bigotimes_{i=1}^m X_i = \operatorname{span}\left\{\bigotimes_{i=1}^m x_i \quad \text{such that} \quad x_i \in X_i \quad \forall i = 1 \ldots m\right\}.$$

By considering the sets $X_1, \ldots, X_m$ of definition 2.2 to be Banach spaces, it is possible to introduce a Banach structure on the product space.

Definition 2.3 (Projective norm) *Let $X_1, \ldots, X_m$ be Banach spaces, each one provided with the norm $\|\cdot\|_{X_i}$ for $i = 1 \ldots m$. By definition, every element u of $\bigotimes_{i=1}^m X_i$ can be written as a finite sum of tensor products: $u = \sum_{j=1}^N x_1^j \otimes \ldots \otimes x_m^j$, but such representation is not necessarily unique. Let $\pi(\cdot)$ be the following real mapping, defined on $\bigotimes_{i=1}^m X_i$:*

$$\pi(u) = \inf \left\{ \sum_{j=1}^{N} \left(\prod_{i=1}^{m} \left\| x_i^j \right\|_{X_i} \right) \quad : \quad u = \sum_{j=1}^{N} x_1^j \otimes \ldots \otimes x_m^j \right\}. \tag{1}$$

*The function $\pi(\cdot)$ is called **projective norm**.*

The function $\pi : \bigotimes_{i=1}^m X_i \to \mathbb{R}$ is indeed a norm on $\bigotimes_{i=1}^m X_i$ as showed by the following proposition, extending Proposition 2.1 of [23].

Proposition 2.2 *Let $X_1, \ldots, X_m$ be Banach spaces. Then, the function $\pi(\cdot)$ defined in eq. (1) is a norm on $\bigotimes_{i=1}^m X_i$. Moreover, $\pi\left(\bigotimes_{i=1}^m x_i\right) = \prod_{i=1}^m \|x_i\|_{X_i}$ for any choice of $(x_1, \ldots, x_m) \in \prod_{i=1}^m X_i$.*

The proof is reported in section A.1.

Definition 2.4 (Projective product space) *The completion of the normed vector space $\bigotimes_{i=1}^m X_i$ with respect to the projective norm $\pi(\cdot)$ defined in definition 2.3 is the **projective product space**, which is a Banach space and is denoted as $\widehat{\bigotimes}_{\pi,i=1}^m X_i$.*

Definition 2.5 (Class of continuous multilinear functional) *We denote the set of **real bounded multilinear functionals** defined on the Banach spaces $X_1, \ldots, X_m$ as $\mathfrak{P}_m(X_1, \ldots, X_m)$.*

As stated in section 1.2 of [23], a primary purpose of the tensor product is the linearization of bilinear mappings. A significant result for Banach spaces is *Theorem 2.9* of [23]. With the following result, we extend the linearization properties of *Theorem 2.9* of [23] to bounded multilinear functionals, while ensuring the continuity with respect to the topology defined by the norm $\pi(\cdot)$.

Proposition 2.3 (Linearization of bounded multilinear functionals) *Let us consider a real-valued, bounded, multilinear functional $P_m : \prod_{i=1}^m X_i \to \mathbb{R}$ defined on the Banach spaces $X_1, \ldots, X_m$. For any Banach space B, we denote B^* its topological dual. Then, there exists a unique linear functional $\widehat{P_m} : \widehat{\bigotimes}_{\pi,i=1}^m X_i \to \mathbb{R}$ such that:*

1. *the functional $\widehat{P_m}$ is continuous, and $\left\|\widehat{P_m}\right\|_{\mathrm{OP}} = \sup_{\|x_i\|_X = 1 \, \forall i} |P_m(x_1, \ldots, x_m)| = \|P_m\|_{\mathrm{OP}}$;*
2. *for all $(x_1, \ldots, x_m) \in \prod_{i=1}^m X_i$, $\widehat{P_m}\left(\bigotimes_{i=1}^m x_i\right) = P_m(x_1, \ldots, x_m)$.*

Moreover, the correspondence $P_m \leftrightarrow \widehat{P_m}$ *is an isometric isomorphism between the Banach spaces* $\mathfrak{P}_m(X_1, \ldots, X_m)$ *and* $\left(\widehat{\bigotimes}_{\pi,i=1}^{m} X_i\right)^*$.

The proof is an immediate application of the Hahn-Banach extension theorem (presented as *Theorem 1.6.1* in [24]), and is reported in section A.2.

2.3 Modeling of the uncertainties

Let us consider the following measure space $(\mathcal{O}, \mathbb{F}, \mathbb{P})$, where $\mathcal{O}$ is the event space, $\mathbb{F}$ a σ-algebra on $\mathcal{O}$, and $\mathbb{P}$ a probability measure, and let $(X, \|\cdot\|_X)$ be a Banach space. In order to model the uncertainties in the model, we use the formalism of Bochner spaces, which extends the theory of integration to Banach-valued functions (see Chapter 1 of [25]).

We recall the definition of measurable and integrable functions in the context of Bochner spaces for a generic measure μ on the σ-algebra $\mathbb{F}$.

Definition 2.6 (μ-simple and strongly μ-measurable functions) *A function* $g : \mathcal{O} \to X$ *is said to be* ***μ-simple*** *if it can be written in the form*

$$\sum_{i=1}^{N} \chi_{A_i} \mathbf{x}_i,$$

where N *is a finite positive integer,* $\mathbf{x}_i \in X$, $A_i \in \mathbb{F}$, *and* $\mu(A_i) < \infty$ *for all* $i \in \{1, \ldots, N\}$, *and* χ_A *is the characteristic function for the set* A.

A function $f : \mathcal{O} \to X$ *is said to be* ***strongly μ-measurable*** *if there exists a sequence* $\{g_i\}_{i=1}^{\infty}$ *of* μ *-simple functions converging to* f μ*-almost everywhere.*

Definition 2.7 (Bochner integral) *The* ***Bochner integral*** *of a simple function* $g = \sum_{i=1}^{N} \chi_{A_i} \mathbf{x}_i : \mathcal{O} \to X$ *with respect to the measure* μ *is defined as*

$$\int_{\mathcal{O}} g \, \mathrm{d}\mu = \sum_{i=1}^{N} \mu(A_i) \, \mathbf{x}_i \quad \in X.$$

A strongly μ*-measurable function* f *is* ***Bochner integrable*** *with respect to the measure* μ *if there exists a sequence* $\{g_i\}_{i=1}^{\infty}$ *of* μ*-simple functions* $g_i : \mathcal{O} \to X$ *such that*

$$\lim_{i \to \infty} \int_{\mathcal{O}} \|f - g_i\|_X \, \mathrm{d}\mu = 0,$$

where the (real) integral has to be intended at the sense of Lebesgue. The ***Bochner integral*** *of such Bochner integrable function function is defined as*

$$\int_{\mathcal{O}} f \, \mathrm{d}\mu = \lim_{i \to \infty} \int_{\mathcal{O}} g_i \, \mathrm{d}\mu \quad \in X.$$

Once defined the integration for Banach-valued functions, we can introduce the Bochner spaces as the equivalent of the usual L^p spaces for real-valued functions.

Definition 2.8 (Bochner spaces and equivalence) *A Bochner integrable function $f : \mathcal{O} \to X$ belongs to the space $\mathcal{L}^p(\mathcal{O}, \mu;\ X)$ for $i \leq p < \infty$ if and only if $\int_{\mathcal{O}} \|f\|_X^p \, \mathrm{d}\mu < \infty$.*

A Bochner integrable function $f : \mathcal{O} \to X$ belongs to the space $\mathcal{L}^\infty(\mathcal{O}, \mu;\ X)$ if and only if there exist a real positive number $r < \infty$ such that $\mu(\{\Omega \in \mathcal{O} : \|f\|_X \geq r\}) = 0$.

*Two strongly μ -measurable function f and g are said to be **equivalent** if the subset of $\mathcal{O}$ where $f \neq g$ has measure 0. The equivalence relation is denoted as $f \sim g$.*

*The **Bochner space** $\mathrm{L}^p(\mathcal{O}, \mu;\ X)$ for $1 \leq p \leq \infty$ is defined as the quotient of $\mathcal{L}^p(\mathcal{O}, \mu;\ X)$ with respect to the equivalence relation "$\sim$".*

Bochner spaces are also Banach spaces with respect to the following norms:

$$\|f\|_p = \left(\int_{\mathcal{O}} \|f\|_X^p \, \mathrm{d}\mu \right)^{1/p} \qquad \text{for} \quad 1 \leq p < \infty;$$

$$\|f\|_\infty = \inf \{ r \geq 0 : \mu(\{\Omega \in \mathcal{O} : \|f\|_X \geq r\}) = 0 \}.$$

Having stated the main definition about generic Bochner spaces, let us focus on the case where we consider a probability measure $\mathbb{P}$. At first, we can remark the following embedding of Bochner spaces.

Proposition 2.4 (Embeddings in Bochner spaces) *Let $(\mathcal{O}, \mathbb{F}, \mathbb{P})$ be a probability space, X a Banach space, and $1 \leq \ell < m < \infty$. Then, the following inclusion is true:*

$$\mathrm{L}^m(\mathcal{O}, \mathbb{P};\ X) \subset \mathrm{L}^\ell(\mathcal{O}, \mathbb{P};\ X).$$

In particular, if $f \in \mathrm{L}^m(\mathcal{O}, \mathbb{P};\ X)$, then f belongs also to $\mathrm{L}^1(\mathcal{O}, \mathbb{P};\ X)$.

Proof The proof relies simply on Hölder's inequality (see *eq. 1.9* of [26]). Let us denote $p = \frac{m}{l}$ and q its conjugate such that $\frac{1}{p} + \frac{1}{q} = 1$. Then, we have:

$$\int_{\mathcal{O}} \|f\|_X^l \, \mathrm{d}\mu = \int_{\mathcal{O}} \|f\|_X^l \, 1 \, \mathrm{d}\mu = \left(\int_{\mathcal{O}} \|f\|_X^{l \frac{m}{l}} \, \mathrm{d}\mu \right)^{1/p} \left(\int_{\mathcal{O}} 1 \, \mathrm{d}\mu \right)^{1/q}$$
$$= \|f\|_{\mathrm{L}^m(\mathcal{O}, \mathbb{P};\ X)}^l \, 1 < \infty.$$

□

We recall the definition of the expectation operator in Bochner spaces and the classical Hille's theorem about the commutation of the expectation and a closed linear operator.

Definition 2.9 (Expectation) *Let $(\mathcal{O}, \mathbb{F}, \mathbb{P})$ be a probability space, and X a Banach space. The **expectation operator** $\mathbb{E}[\,\cdot\,] : \mathrm{L}^1(\mathcal{O}, \mathbb{P};\ X) \to X$ is the bounded linear operator such that, for all $f \in \mathrm{L}^1(\mathcal{O}, \mathbb{P};\ X)$,*

$$\mathbb{E}[f] = \int_{\mathcal{O}} f \, \mathrm{d}\mathbb{P} \quad \in X.$$

Theorem 2.5 (Hille) *Let $f : \mathcal{O} \to X$ be a Bochner-integrable function valued in the Banach space X, and let T be a closed linear operator whose domain $D(T)$ is a subspace of X and has values in another Banach space Y. We suppose that f takes its values in $D(T)$ almost everywhere and the almost everywhere defined function $Tf : \mathcal{O} \to Y$ is Bochner-integrable. Then, f is Bochner-integrable as a $D(T)$-valued function (i.e. the equivalence class of f belongs to $\mathrm{L}^1(\mathcal{O}, \mathbb{P};\ D(T))$), $\mathbb{E}[f] \in D(T)$, and*

$$\mathbb{E}[T f] = T\,\mathbb{E}[f].$$

Hille's theorem is reported as Theorem 1.2.4 in [25]. We can remark that Hille's theorem is valid if T is a continuous operator, since all continuous operator is closed (see the definition of closed operator at page 15 of [25]). However, Proposition 1.2.3 and Equation (1.2) of [25] point out that, for continuous operators, it is not necessary to prove Hille's theorem to get the same properties, since they descend directly from the definition of Bochner integral.

3 Main results

3.1 Correlation operator and multilinear functionals

Having introduced the concepts of tensor product between Banach spaces and of Bochner-integrability, we combine the results of section 2.2 and section 2.3, and introduce the correlation operator for multilinear functionals under uncertainties. The correlation operator has been studied in the context of shape optimization under uncertainties in [20], limitedly to bilinear functionals defined on Hilbert spaces. First of all, we can state a result about the Bochner-integrability of the tensor product.

Proposition 3.1 *Let $X_1, \dots, X_m$ be Banach spaces endowed with the norms $\|\cdot\|_{X_i}$ for $i = 1, \dots, m$. Let us consider $x_1, \dots, x_m$, each belonging to the Bochner space $\mathrm{L}^m(\mathcal{O}, \mathbb{P};\ X_i)$. Finally, we define the mapping $\omega \mapsto \bigotimes_{i=1}^m x_i(\omega)$ from the event space $\mathcal{O}$ to the Banach space $\widehat{\bigotimes}_{\pi,i=1}^m X_i$. Then, such function belongs to the Bochner space $\mathrm{L}^1\left(\mathcal{O}, \mathbb{P};\ \widehat{\bigotimes}_{\pi,i=1}^m X_i\right)$.*

Proof In order to prove that $\bigotimes_{i=1}^m x_i(\cdot) \in \mathrm{L}^1\left(\mathcal{O}, \mathbb{P};\ \widehat{\bigotimes}_{\pi,i=1}^m X_i\right)$, we estimate its norm as stated in definition 2.8, and we use Hölder's inequality extended to multiple terms:

$$\begin{aligned}\int_{\mathcal{O}} \pi\left(\bigotimes_{i=1}^m x_i(\omega)\right) \mathrm{d}\mathbb{P}(\omega) &= \int_{\mathcal{O}} \left(\prod_{i=1}^m \|x_i(\omega\|_{X_i}\right) \mathrm{d}\mathbb{P}(\omega) \\ &\leq \prod_{i=1}^m \left(\int_{\mathcal{O}} \|x_i(\omega)\|_{X_i}\right) \mathrm{d}\mathbb{P}(\omega) = \prod_{i=1}^m \|x_i\|_{\mathrm{L}^m(\mathcal{O},\mathbb{P};\, X_i)} < \infty.\end{aligned}$$

□

Next, the correlation operator is introduced. As it is remarked in [20], the literature is not consistent in the definition of the correlation between random variables. In this paper, we adopt the following definition.

Definition 3.1 (Correlation operator on Bochner spaces) *Let $(\mathcal{O}, \mathbb{F}, \mathbb{P})$ be a probability space, and $\left(X_i, \|\cdot\|_{X_i}\right)$ Banach spaces for $i = 1, \dots, m$. Let us consider the operator $\tilde{C}_m(\cdot)$ defined on $\prod_{i=1}^m \mathrm{L}^m(\mathcal{O}, \mathbb{P};\ X_i)$, mapping $(x_1(\cdot), \dots, x_m(\cdot))$ to the operator $\mathcal{O} \ni \omega \mapsto \bigotimes_{i=1}^m x_i(\omega)$. Let us denote $C_m(x_1, \dots, x_m)$ the equivalence class of $\tilde{C}_m(x_1, \dots, x_m)$ with respect to the relation "$\sim$". Thanks to proposition 3.1, we know that the function $C_m(x_1, \dots, x_m)$ is Bochner-integrable.*

*The **correlation** between the m functions $x_1, \dots, x_m$ is defined as*

$$\mathrm{Cor}_m(x_1, \dots, x_m) = \mathbb{E}\left[C_m(x_1, \dots, x_m)\right] \in \widehat{\bigotimes_{i=1}^m}_{\pi} X_i,$$

*and the **correlation operator** $\mathrm{Cor}_m : \prod_{i=1}^m \mathrm{L}^m(\mathcal{O}, \mathbb{P};\ X_i) \to \widehat{\bigotimes}_{\pi,i=1}^m X_i$ is a bounded linear operator associating m random vectors to their correlation.*

Finally, we state a proposition that allows the expression of the expected value of a multilinear expression in terms of a correlation tensor.

Proposition 3.2 *Let $(\mathcal{O}, \mathbb{F}, \mathbb{P})$ be a probability space, $X_1, \dots, X_m$ Banach spaces provided with the norms $\|\cdot\|_{X_i}$ for $i = 1 \dots m$, and $P_m : \prod_{i=1}^m X_i \to \mathbb{R}$ a bounded multilinear operator. Then, there exists a unique bounded, real-valued, linear operator $\widehat{P_m}$ defined on $\widehat{\bigotimes}_{\pi,i=1}^m X_i$ such that these three statements hold true for all $(x_1, \dots, x_m) \in \prod_{i=1}^m \mathrm{L}^m(\mathcal{O}, \mathbb{P};\ X_i)$:*

1. $P_m(x_1, \dots, x_m) \in \mathrm{L}^1(\mathcal{O}, \mathbb{P})$,
2. $P_m(x_1(\omega), \dots, x_m(\omega)) = \widehat{P_m}\left(\tilde{C}_m(x_1, \dots, x_m)(\omega)\right)$, *for almost all* $\omega \in \mathcal{O}$,
3. $\mathbb{E}\left[P_m(x_1, \dots, x_m)\right] = \widehat{P_m}\left(\mathrm{Cor}_m(x_1, \dots, x_m)\right)$.

Proof The first point comes directly from the continuity of the operator P_m and the application of Hölder's inequality. The second can be deduced from proposition 2.3.

In order to prove the third point, we show that the three hypotheses of Hille's theorem (theorem 2.5) are verified. The function $\omega \mapsto P_m(x_1(\omega), \dots, x_m(\omega))$ is Bochner-integrable thanks to proposition 3.1. The operator $\widehat{P_m}$ is closed since it is continuous, as proved by the second point of this proposition. Moreover, the function $\widehat{P_m}\left(C_m(x_1, \dots, x_m)(\omega)\right)$ is Bochner-integrable as well, thanks to points 1 and 2. Therefore, we can apply theorem 2.5 and conclude:

$$\begin{aligned}\mathbb{E}\left[P_m(x_1, \dots, x_m)\right] &= \mathbb{E}\left[\widehat{P_m}(C(x_1, \dots, x_m))\right] \\ &= \widehat{P_m}\left(\mathbb{E}\left[C(x_1, \dots, x_m)\right]\right) = \widehat{P_m}\left(\mathrm{Cor}_m(x_1, \dots, x_m)\right).\end{aligned}$$

□

3.2 Shape optimization with uncertain parameters

Let $\mathcal{S}_{adm}$ be a set of admissible bounded domains in $\mathbb{R}^d$, $(\mathcal{O}, \mathbb{F}, \mathbb{P})$ a probability space, and $(Y, \|\cdot\|_Y)$ a Banach space. We consider $\mathbf{g} \in \mathrm{L}^m(\mathcal{O}, \mathbb{P};\ Y)$ to be a Bochner-integrable random variable, and we are interested in the solution of the following shape optimization problem:

$$\begin{cases} \text{Find } \Omega_{opt} \in \mathcal{S}_{adm} \\ \text{minimizing } \Omega \mapsto \mathbb{E}\left[\mathcal{J}(\Omega, \mathbf{g})\right] = \mathbb{E}\left[P_m^{\Omega}(\mathbf{g}, \cdots, \mathbf{g})\right]. \end{cases} \tag{2}$$

We consider $P_m^{\Omega} : \prod_{i=1}^m Y \to \mathbb{R}$ to be a bounded m-multilinear functional, such that $P_m^{\Omega}(\mathbf{g}_1, \ldots, \mathbf{g}_m)$ is Fréchet differentiable at any $\Omega \in \mathcal{S}_{adm}$ for any choice of $(\mathbf{g}_1, \ldots, \mathbf{g}_m) \in Y^m$.

In order to be able to solve problem (2) using Hadamard's shape variation method, we need to compute the shape derivative of the functional $\Omega \mapsto \mathbb{E}\left[\mathcal{J}(\Omega, \mathbf{g})\right]$. Similarly to the procedure adopted in [20], we look for a deterministic expression of $\mathbb{E}\left[\mathcal{J}(\Omega, \mathbf{g})\right]$ using the correlation operator. Through proposition 3.2, we find that there exists a continuous linear operator $\widehat{P_m^{\Omega}} \in \left(\widehat{\bigotimes}_{\pi,i=1}^m Y\right)^*$ such that, for all $\mathbf{g} \in \mathrm{L}^m(\mathcal{O}, \mathbb{P};\ Y)$, the following identity holds:

$$\mathbb{E}\left[P_m^{\Omega}(\mathbf{g}, \cdots, \mathbf{g})\right] = \widehat{P_m^{\Omega}}\left(\mathrm{Cor}(\mathbf{g}, \cdots, \mathbf{g})\right). \tag{3}$$

In [20], the authors propose the decomposition of the correlation tensor using the Karhunen-Loève expansion, as described in section 2.3.1 of [27]. However, such decomposition applies only for symmetrical bilinear functionals, where the space Y has a Hilbertian structure. Indeed, the Karhunen-Loève expansion is a direct application of the spectral theorem, and it does not apply when an inner product cannot be defined (see *Theorem 6.73* of [26] for reference).

In order to be able to decompose the tensor $\mathrm{Cor}(\mathbf{g}, \cdots, \mathbf{g})$, some further hypotheses on the random variable are necessary. Assuming that $\mathbf{g}$ can be written as follows:

$$\mathbf{g}(\cdot) = \sum_{k=1}^{N} \mathbf{g}_i\, \xi_i(\cdot) \tag{4}$$

with $N > 0$ integer, $\mathbf{g}_1, \ldots, \mathbf{g}_N \in Y$ deterministic terms, and $\xi_1, \ldots, \xi_N \in \mathrm{L}^m(\mathcal{O}, \mathbb{P};\ \mathbb{R})$ real valued random variables. By construction, $\mathbf{g} \in \mathrm{L}^m(\mathcal{O}, \mathbb{P};\ Y)$, and $C_m(\mathbf{g}, \ldots, \mathbf{g}) \in \mathrm{L}^1\left(\mathcal{O}, \mathbb{P};\ \widehat{\bigotimes}_{\pi,i=1}^m Y\right)$ thanks to proposition 3.1. Thus, the correlation tensor $\mathrm{Cor}(\mathbf{g}, \ldots, \mathbf{g})$ is a well-defined element of $\widehat{\bigotimes}_{\pi,i=1}^m Y$, and can be expressed as:

$$\mathrm{Cor}(\mathbf{g}, \ldots, \mathbf{g}) = \mathbb{E}\left[\left(\sum_{k_1=1}^{N} \mathbf{g}_{k_1} \xi_{k_1}\right) \otimes \ldots \otimes \left(\sum_{k_m=1}^{N} \mathbf{g}_{k_m} \xi_{k_m}\right)\right]$$

$$= \mathbb{E}\left[\sum_{\vec{\mathbf{k}}\in\{1,\dots,N\}^m}\left[\left(\prod_{i=1}^m \xi_{k_i}\right)\left(\bigotimes_{i=1}^m \mathbf{g}_{k_i}\right)\right]\right]$$

$$= \sum_{\vec{\mathbf{k}}\in\{1,\dots,N\}^m}\left(\mathbb{E}\left[\prod_{i=1}^m \xi_{k_i}\right]\bigotimes_{i=1}^m \mathbf{g}_{k_i}\right). \quad (5)$$

The expression of eq. (5) can be further simplified if the random variables $\xi_1,\dots,\xi_N$ are considered independent. Let us introduce the following notation:

Definition 3.2 *Given a m-uple of integers $\vec{\mathbf{k}} = (k_1,\dots,k_m)$ and an integer j, we denote $C^j_{\vec{\mathbf{k}}}$ the number of times the integer j appears in the m-uple $\vec{\mathbf{k}}$. In other terms, $C^j_{\vec{\mathbf{k}}}$ identifies the following cardinality:*

$$C^j_{\vec{\mathbf{k}}} = \mathrm{Card}\left\{i \in \{1,\dots,m\} \text{ such that } k_i = j\right\}.$$

If the random variables are independent, the expression eq. (5) can be written as follows, highlighting the moments of any single variable:

$$\mathrm{Cor}\left(\mathbf{g},\dots,\mathbf{g}\right) = \sum_{\vec{\mathbf{k}}\in\{1,\dots,N\}^m}\left\{\prod_{j=1}^N\left(\mathbb{E}\left[\xi_j^{C^j_{\vec{\mathbf{k}}}}\right]\right)\bigotimes_{i=1}^m \mathbf{g}_{k_i}\right\}. \quad (6)$$

Further simplifications can be done imposing stricter hypotheses on the distributions of the ξ_j (symmetry, normality, etc...).

Now that a decomposition for the correlation tensor has been found, we use proposition 2.3, and the expression eq. (6) of the correlation in order to express the functional $\Omega \mapsto \mathbb{E}\left[\mathcal{J}\left(\Omega,\mathbf{g}\right)\right]$ as a deterministic function. For any $\boldsymbol{\theta} \in \mathrm{W}^{1,\infty}\left(\mathbb{R}^d,\mathbb{R}^d\right)$, we have:

$$\begin{aligned}
\mathbb{E}\left[\mathcal{J}\left(\Omega,\mathbf{g}\right)\right] &= \mathbb{E}\left[P_m^\Omega(\mathbf{g},\dots,\mathbf{g})\right] = \widehat{P_m^\Omega}\left(\mathrm{Cor}\left(\mathbf{g},\cdots,\mathbf{g}\right)\right) \\
&= \widehat{P_m^\Omega}\left(\sum_{\vec{\mathbf{k}}\in\{1,\dots,N\}^m}\left\{\prod_{j=1}^N\left(\mathbb{E}\left[\xi_j^{C^j_{\vec{\mathbf{k}}}}\right]\right)\bigotimes_{i=1}^m \mathbf{g}_{k_i}\right\}\right) \\
&= \sum_{\vec{\mathbf{k}}\in\{1,\dots,N\}^m}\left\{\prod_{j=1}^N\left(\mathbb{E}\left[\xi_j^{C^j_{\vec{\mathbf{k}}}}\right]\right)\widehat{P_m^\Omega}\left(\bigotimes_{i=1}^m \mathbf{g}_{k_i}\right)\right\} \\
&= \sum_{\vec{\mathbf{k}}\in\{1,\dots,N\}^m}\left\{\prod_{j=1}^N\left(\mathbb{E}\left[\xi_j^{C^j_{\vec{\mathbf{k}}}}\right]\right)P_m^\Omega\left(\mathbf{g}_{k_1},\dots,\mathbf{g}_{k_1}\right)\right\}.
\end{aligned} \quad (7)$$

Therefore, thanks to the linearity of the shape derivative, we find:

$$\frac{\mathrm{d}}{\mathrm{d}\Omega}\mathbb{E}\left[\mathcal{J}\left(\Omega,\mathbf{g}\right)\right](\boldsymbol{\theta}) = \frac{\mathrm{d}}{\mathrm{d}\Omega}\mathbb{E}\left[P_m^\Omega(\mathbf{g},\dots,\mathbf{g})\right](\boldsymbol{\theta})$$
$$= \sum_{\vec{\mathbf{k}}\in\{1,\dots,N\}^m}\left\{\prod_{j=1}^{N}\left(\mathbb{E}\left[\xi_j^{C_{\vec{\mathbf{k}}}^j}\right]\right)\frac{\mathrm{d}}{\mathrm{d}\Omega}\left[P_m^\Omega\left(\mathbf{g}_{k_1},\dots,\mathbf{g}_{k_1}\right)\right](\boldsymbol{\theta})\right\}. \quad (8)$$

Let us denote $\mathcal{T}\left(P_m^\Omega, N\right)$ the minimal number of terms to be computed in eq. (7) and eq. (8) to express the expected value of the functional and its derivative. In the most general case, $\mathcal{T}\left(P_m^\Omega, N\right) = N^m$, since we have to compute all the terms in the form $P_m^\Omega\left(\mathbf{g}_{k_1},\dots,\mathbf{g}_{k_1}\right)$, as well as their shape derivatives. However, such number can be reduced if the multilinear functional P_m^Ω shows some symmetries among its arguments. Indeed, if P_m^Ω is completely commutative, we have $\mathcal{T}\left(P_m^\Omega, N\right) = \binom{N+m-1}{m}$.

3.3 Uncertain loads in linear elasticity

Often, before computing the value of the objective functional in an optimization problem, it is necessary to pass through an intermediary step that is the computation of the state of the system. For any $\Omega \in \mathcal{S}_{adm}$, let $(X^\Omega, \|\cdot\|_{X^\Omega})$ be a Banach space, and $\mathcal{A}_\Omega : X^\Omega \to Y$ a bounded, linear, invertible functional. Let us consider the following optimization problem:

$$\begin{cases}\text{Find } \Omega_{opt} \in \mathcal{S}_{adm}\\ \text{minimizing } \Omega \mapsto \mathbb{E}\left[\mathcal{J}\left(\Omega,\mathbf{g}\right)\right] = \mathbb{E}\left[Q_m^\Omega(\mathbf{u}_\Omega,\cdots,\mathbf{u}_\Omega)\right],\\ \text{where } \mathcal{A}_\Omega\,\mathbf{u}_\Omega(\omega) = \mathbf{g}(\omega) \quad \text{for all } \omega \in \mathcal{O},\end{cases} \quad (9)$$

where $Q_m^\Omega : \prod_{i=1}^m X^\Omega \to \mathbb{R}$ is a bounded m-multilinear functional. The term $\mathbf{u}(\cdot)$ is said to be the state of the system. The state equation $\mathcal{A}_\Omega\,\mathbf{u}_\Omega = \mathbf{g}$ can be interpreted as a constraint in the optimization problem, and might require the solution of a partial differential equation. We remark that, since $\mathbf{g}(\cdot) \in \mathrm{L}^m\left(\mathcal{O},\mathbb{P};\ Y\right)$ is a random variable, $\mathbf{u}_\Omega(\cdot)$ is a random variable as well, and it belongs to the Bochner space $\mathrm{L}^m\left(\mathcal{O},\mathbb{P};\ X^\Omega\right)$.

From now on, we focus on shape optimization problems in the context of linear elasticity, in which case we adopt as X^Ω the space $\mathrm{W}^{1,m}\left(\Omega,\mathbb{R}^d\right) \cap \mathbf{H}^1\left(\Omega,\mathbb{R}^d\right)$. Further information on the theory of linear elasticity can be found in [28] and in [29].

Definition 3.3 (Strain and stress tensors) *Let us consider the two* ***Lamé coefficients*** λ *and* μ *such that the quantities* μ, *and* $2\mu + d\lambda$ *are strictly positive. For any* $\mathbf{v} \in \mathbf{H}^1\left(\mathbb{R}^d,\mathbb{R}^d\right)$, *representing a displacement field, the* ***infinitesimal strain tensor*** $\boldsymbol{\varepsilon}\left(v\right)$ *is defined as* $\boldsymbol{\varepsilon}\left(v\right) = \frac{\nabla\mathbf{v}+(\nabla\mathbf{v})^T}{2}$. *The* ***Cauchy stress tensor*** $\boldsymbol{\sigma}\left(\mathbf{v}\right)$ *is defined as the following linear application of the strain tensor:*

$$\boldsymbol{\sigma}\left(\mathbf{v}\right) = A\boldsymbol{\varepsilon}\left(\mathbf{v}\right) = 2\mu\boldsymbol{\varepsilon}\left(\mathbf{v}\right) + \lambda(\mathrm{div}\,\mathbf{v}).$$

We consider the following shape optimization problem, restriction of eq. (9) to the case of linear elasticity:

$$\left|\begin{array}{l}\text{Find } \Omega_{opt} \in \mathcal{S}_{adm} \\ \text{minimizing } \Omega \mapsto \mathbb{E}\left[\mathcal{J}\left(\Omega, \mathbf{g}\right)\right] = \mathbb{E}\left[Q_m^{\Omega}(\mathbf{u}_\Omega, \cdots, \mathbf{u}_\Omega)\right], \\ \text{where, for all } \omega \in \mathcal{O}, \text{ the state } \mathbf{u}_\Omega \in \left[\mathrm{H}^1(\Omega)\right]^d \text{ solves:} \\ \qquad \left\{\begin{array}{rll} -\mathrm{div}\,\boldsymbol{\sigma}\left(\mathbf{u}_\Omega\right) &= \mathbf{0} & \text{in } \Omega, \\ \boldsymbol{\sigma}\left(\mathbf{u}_\Omega(\omega)\right)\mathbf{n} &= \mathbf{g}(\omega) & \text{on } \Gamma_{\mathrm{N}}, \\ \boldsymbol{\sigma}\left(\mathbf{u}_\Omega(\omega)\right)\mathbf{n} &= \mathbf{0} & \text{on } \Gamma_0, \\ \mathbf{u}_\Omega(\omega) &= \mathbf{0} & \text{on } \Gamma_{\mathrm{D}}. \end{array}\right. \end{array}\right. \tag{10}$$

In problem (10) we denote Γ_{N}, Γ_0 and Γ_{D} three open disjointed portions of the border of Ω with strictly positive measure such that $\overline{\Gamma_{\mathrm{N}}} \cup \overline{\Gamma_0} \cup \overline{\Gamma_{\mathrm{D}}} = \partial\Omega$.

The problem defining the state equation can be written in variational form:

$$\left|\begin{array}{l}\text{Find } \mathbf{u}_\Omega \in V = \left\{\mathbf{v} \in \mathrm{H}^1(\Omega)^d : \mathbf{v} = \mathbf{0} \text{ on } \Gamma_{\mathrm{D}}\right\} \text{ such that} \\ \text{for all } \mathbf{v} \in V \\ \displaystyle\int_\Omega \left(\boldsymbol{\sigma}\left(\mathbf{u}_\Omega\right) : \boldsymbol{\varepsilon}\left(\mathbf{v}\right)\right) \mathrm{d}\mathbf{x} = \int_{\Gamma_{\mathrm{N}}} \mathbf{g}(\Omega) \cdot \mathbf{v}\, \mathrm{d}\mathbf{s}. \end{array}\right. \tag{11}$$

For simplicity, we suppose that all admissible shapes in $\mathcal{S}_{adm}$ share the portions Γ_{N} and Γ_{D}, constraining the displacements fields $\boldsymbol{\theta} \in \Theta_{adm} \subset \mathrm{W}^{1,\infty}\left(\mathbb{R}^d, \mathbb{R}^d\right)$ to be equal to 0 on these surfaces. We suppose also that the admissibles domains $\Omega \in \mathcal{S}_{adm}$ are regular enough to assure that $\mathbf{u}_\Omega \in \mathrm{W}^{1,m}\left(\Omega, \mathbb{R}^d\right) \cap \mathbf{H}^1\left(\Omega, \mathbb{R}^d\right)$. Moreover, we focus our study on functionals Q_m^{Ω} with the following structure:

$$Q_m^{\Omega}(\mathbf{v}_1, \ldots, \mathbf{v}_m) = \int_\Omega q_1(\mathbf{v}_1, \ldots, \mathbf{v}_m)\, \mathrm{d}\mathbf{x} + \int_\Omega q_2(\nabla\mathbf{v}_1, \ldots, \nabla\mathbf{v}_m)\, \mathrm{d}\mathbf{x}, \tag{12}$$

where $q_1(\cdots)$ and $q_2(\cdots)$ are multilinear and continuous. Finally, we introduce the following notation:

- $\mathcal{A}_{(1,m),N} = \{1, \ldots, N\}^m$ is the set of all m-uples whose elements are integers between 1 and N;
- $\mathcal{A}^{i,j}_{(1,m),N} = \left\{\vec{\mathbf{k}} \in \mathcal{A}_{(1,m),N} \text{ such that } k_i = i\right\} \subset \mathcal{A}_{(1,m),N}$ is the subset of all m-uples in $\mathcal{A}_{(1,m),N}$ whose i-th element is equal to j;
- given N real random variables $\xi_1, \ldots, \xi_m$ belonging to the Bochner space $\mathrm{L}^m\left(\mathcal{O}, \mathbb{P};\, \mathbb{R}\right)$ and a m-uple $\vec{\mathbf{k}} = (k_1, \ldots, k_m) \in \mathcal{A}_{(1,m),N}$, we denote $\mu_{i,j}$ the i-th moment of the random variable ξ_j : $\mu_{i,j} = \mathbb{E}\left[\xi_j^i\right]$;
- finally, we denote $\alpha(\vec{\mathbf{k}})$ the following quantity:

$$\alpha(\vec{\mathbf{k}}) = \alpha(k_1, \ldots, k_m) = \prod_{j=1}^{N} \left(\mathbb{E}\left[\xi_j^{C^j_{\vec{\mathbf{k}}}}\right]\right) = \prod_{j=1}^{N} \mu_{C^j_{\vec{\mathbf{k}}}, j}.$$

Proposition 3.3 *Let us consider the optimization problem (10), where the objective functional follows the structure eq. (12). Let $\Omega \in \mathcal{S}_{adm}$ be a $\mathcal{C}^1$ domain. Moreover, let us consider that $\mathbf{g} \in \mathrm{L}^m\left(\mathcal{O}, \mathbb{P};\, \mathrm{L}^2(\Gamma_\mathrm{N})\right)$ can be decomposed as in eq. (4), where the N real random variables $\xi_i \in \mathrm{L}^m\left(\mathcal{O}, \mathbb{P};\, \mathbb{R}\right)$ are mutually independent. Then, we can write the shape derivative of the objective in Ω as follows:*

$$\frac{\mathrm{d}}{\mathrm{d}\Omega}\mathbb{E}\left[\mathcal{J}\left(\Omega, \mathbf{g}\right)\right](\boldsymbol{\theta}) = -\sum_{j=1}^{N}\int_{\Gamma_0}\left(\boldsymbol{\theta}\cdot\mathbf{n}\right)\left(\boldsymbol{\sigma}\left(\mathbf{u}_j\right) : \boldsymbol{\varepsilon}\left(\mathbf{w}_j\right)\right)\mathrm{d}\mathbf{s}$$
$$+\sum_{\vec{\mathbf{k}}\in\mathcal{A}_{(1,m),N}}\left(\alpha(\vec{\mathbf{k}})\int_{\Gamma_0}\left(\boldsymbol{\theta}\cdot\mathbf{n}\right)\left(q_1(\mathbf{u}_{k1},\ldots,\mathbf{u}_{km}) + q_2(\nabla\mathbf{u}_{k1},\ldots,\nabla\mathbf{u}_{km})\right)\mathrm{d}\mathbf{s}\right) \tag{13}$$

where the N states $\mathbf{u}_1,\ldots,\mathbf{u}_N$ solve the state equation for $\mathbf{g}_1,\ldots,\mathbf{g}_N$ respectively, while the N adjoint states $\mathbf{w}_1,\ldots,\mathbf{w}_N$ solve the following adjoint problems:

$$\begin{cases} -\operatorname{div}\boldsymbol{\sigma}\left(\mathbf{w}_j\right) = \sum_{i=1}^{m}\sum_{\vec{\mathbf{k}}\in\mathcal{A}^{i,j}_{(1,m),N}}\alpha(\vec{\mathbf{k}})\left(\frac{\partial q_1}{\partial \mathbf{v}_i}(\mathbf{u}_{k1},\ldots,\mathbf{u}_{km})\right. \\ \qquad\qquad \left. -\ \operatorname{div}\frac{\partial q_2}{\partial \vec{\mathbf{V}}_i}(\nabla\mathbf{u}_{k1},\ldots,\nabla\mathbf{u}_{km})\right) & \text{in } \Omega, \\ \boldsymbol{\sigma}\left(\mathbf{w}_j\right)\mathbf{n} = \sum_{i=1}^{m}\sum_{\vec{\mathbf{k}}\in\mathcal{A}^{i,j}_{(1,m),N}}\alpha(\vec{\mathbf{k}})\left(\frac{\partial q_2}{\partial \vec{\mathbf{V}}_i}(\nabla\mathbf{u}_{k1},\ldots,\nabla\mathbf{u}_{km})\right)^T\mathbf{n} & \text{on } \Gamma_0\cup\Gamma_\mathrm{N}, \\ \mathbf{w}_j = \mathbf{0} & \text{on } \Gamma_\mathrm{D}. \end{cases} \tag{14}$$

The result of proposition 3.3 can be obtained using Céa's rapid derivation method, (see [30] and section 6.4.3 of [4]). Such method is a purely formal procedure and assumes the existence of the Eulerian derivative of the state and the regularity of the domain Ω. Such proof is reported in section 3.4.

It is worth remarking that the method presented in this section requires the computation of only N adjoint states. Moreover, the PDEs defining the states $\mathbf{u}_1,\ldots,\mathbf{u}_N$ and the adjoint states $\mathbf{w}_1,\ldots,\mathbf{w}_N$ all share the structure of their left-hand side. Such property can be very useful for the numerical simulations since, by decomposing once the matrix representing the discretization of the bilinear form $(\mathbf{u},\mathbf{v}) \mapsto \int_\Omega \left(\boldsymbol{\sigma}\left(\mathbf{u}\right) : \boldsymbol{\varepsilon}\left(\mathbf{v}\right)\right)\mathrm{d}\mathbf{x}$, we can solve the $2N$ boundary value problems faster.

3.4 Proof of Proposition 3.3

As first step, we apply the decomposition eq. (7) to the objective functional $\mathbb{E}\left[Q_m^\Omega(\mathbf{u}_\Omega,\cdots,\mathbf{u}_\Omega)\right]$, and we obtain the following expression:

$$\mathbb{E}\left[Q_m^\Omega(\mathbf{u}_\Omega,\cdots,\mathbf{u}_\Omega)\right] = \sum_{\vec{\mathbf{k}}\in\mathcal{A}_{(1,m),N}}\alpha(\vec{\mathbf{k}})\left(\int_\Omega q_1(\mathbf{u}_{k1},\ldots,\mathbf{u}_{km})\,\mathrm{d}\mathbf{x}\right.$$

$$+\int_\Omega q_2(\nabla \mathbf{u}_{k1},\dots,\nabla \mathbf{u}_{km})\,\mathrm{d}\mathbf{x}\Bigg),$$

where, for every $j \in \{1,\dots,N\}$ $\mathbf{u}_j$ solves the state equation for the right-hand side $\mathbf{g}_j$ on the domain Ω.

We introduce the following Lagrangian function $\mathcal{L} : \mathcal{S}_{adm} \times ([\mathrm{H}^1(\mathbb{R}^d)]^d)^N \times ([\mathrm{H}^1(\mathbb{R}^d)]^d)^N \to \mathbb{R}$ associated to problem (10) where the state equation is seen as a PDE constraint:

$$\begin{aligned}\mathcal{L}\left(\Omega,\hat{\mathbf{u}}_1,\dots,\hat{\mathbf{u}}_N,\hat{\mathbf{w}}_1,\dots,\hat{\mathbf{w}}_N\right) = \sum_{\vec{\mathbf{k}}\in\mathcal{A}_{(1,m),N}} \Bigg\{\alpha(\vec{\mathbf{k}})\left(\int_\Omega q_1(\hat{\mathbf{u}}_{k_1},\dots,\hat{\mathbf{u}}_{k_m})\,\mathrm{d}\mathbf{x}\right.\\ \left.+\int_\Omega q_2(\nabla\hat{\mathbf{u}}_{k1},\dots,\nabla\hat{\mathbf{u}}_{km})\right)\mathrm{d}\mathbf{x}\Bigg\} - \sum_{j=1}^{N}\Bigg\{\int_\Omega \left(\boldsymbol{\sigma}\left(\hat{\mathbf{u}}_j\right):\boldsymbol{\varepsilon}\left(\hat{\mathbf{w}}_j\right)\right)\mathrm{d}\mathbf{x}\\ -\int_{\Gamma_\mathrm{N}}\mathbf{g}_j\cdot\hat{\mathbf{w}}_j\,\mathrm{d}\mathbf{s} - \int_{\Gamma_\mathrm{D}}\left(\hat{\mathbf{w}}_j\cdot\left(\boldsymbol{\sigma}\left(\hat{\mathbf{u}}_j\right)\mathbf{n}\right)+\hat{\mathbf{u}}_j\cdot\left(\boldsymbol{\sigma}\left(\hat{\mathbf{w}}_j\right)\mathbf{n}\right)\right)\mathrm{d}\mathbf{s}\Bigg\} \quad (15)\end{aligned}$$

The variables $\hat{\mathbf{w}}_1,\dots,\hat{\mathbf{w}}_N$ act as Lagrange multipliers for the PDE constraints of the terms $\hat{\mathbf{u}}_1,\dots,\hat{\mathbf{u}}_N$. In order to assure that all arguments of the Lagrangian are independent, the terms $\hat{\mathbf{u}}_1,\dots,\hat{\mathbf{u}}_N$ and $\hat{\mathbf{w}}_1,\dots,\hat{\mathbf{w}}_N$ are defined on the whole space $\mathbb{R}^d$, and not only on Ω. The term of eq. (15) defined as an integral on the portion Γ_D of the boundary enforces the Dirichlet boundary condition, which is similar to the proof of *Theorem 7* in [7].

By construction, the terms $\mathbf{u}_1,\dots,\mathbf{u}_N$ solving the equation $\frac{\partial\mathcal{L}}{\partial\hat{\mathbf{w}}_j}=0$, are also solutions of the state equation for the right-hand side $\mathbf{g}=\mathbf{g}_j$. Indeed, for $j=1\dots N$ and for any $\mathbf{v}\in\mathrm{H}^1(\mathbb{R}^d)$:

$$\begin{aligned}0=\frac{\partial\mathcal{L}}{\partial\hat{\mathbf{w}}_j}(\Omega,\mathbf{u}_1,\dots,\mathbf{u}_N,\hat{\mathbf{w}}_1,\dots,\hat{\mathbf{w}}_N)(\mathbf{v}) = -\int_\Omega\left(\boldsymbol{\sigma}\left(\mathbf{u}_j\right):\boldsymbol{\varepsilon}\left(\mathbf{v}\right)\right)\mathrm{d}\mathbf{x}\\ +\int_{\Gamma_\mathrm{N}}\mathbf{g}_j\cdot\mathbf{v}\,\mathrm{d}\mathbf{s}+\int_{\Gamma_\mathrm{D}}\left(\mathbf{v}\cdot\left(\boldsymbol{\sigma}\left(\mathbf{u}_j\right)\mathbf{n}\right)+\mathbf{u}_j\cdot\left(\boldsymbol{\sigma}\left(\mathbf{v}\right)\mathbf{n}\right)\right)\mathrm{d}\mathbf{s}\\ =\int_\Omega\left(\mathrm{div}\left(\boldsymbol{\sigma}\left(\mathbf{u}_j\right)\right)\right)\cdot\mathbf{v}\,\mathrm{d}\mathbf{x}+\int_{\Gamma_\mathrm{N}}\left(\mathbf{g}_j-\boldsymbol{\sigma}\left(\mathbf{u}_j\right)\mathbf{n}\right)\cdot\mathbf{v}\,\mathrm{d}\mathbf{s}+\int_{\Gamma_\mathrm{D}}\left(\mathbf{u}_j\cdot\left(\boldsymbol{\sigma}\left(\mathbf{v}\right)\mathbf{n}\right)\right)\mathrm{d}\mathbf{s}.\end{aligned}$$

The state equations for $\mathbf{u}_j$ are derived by choosing a test function with compact support in Ω, and the boundary conditions by variating the trace of $\mathbf{v}$ on Γ_N and the normal stress $\boldsymbol{\sigma}(\mathbf{v})\mathbf{n}$ on Γ_D.

Thanks to this result and to the linearity of the state equation, we can express the functional $\mathbb{E}\left[Q_m^\Omega(\mathbf{u}_\Omega,\cdots,\mathbf{u}_\Omega)\right]$ in terms of the Lagrangian:

$$\mathbb{E}\left[Q_m^\Omega(\mathbf{u}_\Omega,\cdots,\mathbf{u}_\Omega)\right]=\mathcal{L}\left(\Omega,\mathbf{u}_1,\dots,\mathbf{u}_N,\hat{\mathbf{w}}_1,\dots,\hat{\mathbf{w}}_N\right), \quad (16)$$

for all $\hat{\mathbf{w}}_1,\dots,\hat{\mathbf{w}}_N\in\mathrm{H}^1(\mathbb{R}^d)$.

The expression for the shape derivative of the functional of interest is found differentiating eq. (16) with respect to Ω:

$$\begin{aligned}\frac{\mathrm{d}}{\mathrm{d}\Omega}\mathbb{E}\left[Q_m^\Omega(\mathbf{u}_\Omega,\cdots,\mathbf{u}_\Omega)\right](\boldsymbol{\theta}) &= \frac{\mathrm{d}}{\mathrm{d}\Omega}\mathcal{L}\left(\Omega,\mathbf{u}_1,\ldots,\mathbf{u}_N,\hat{\mathbf{w}}_1,\ldots,\hat{\mathbf{w}}_N\right)\\ &= \frac{\partial\mathcal{L}}{\partial\Omega}\left(\Omega,\mathbf{u}_1,\ldots,\mathbf{u}_N,\hat{\mathbf{w}}_1,\ldots,\hat{\mathbf{w}}_N\right)(\boldsymbol{\theta})\\ &\quad+\sum_{j=1}^{N}\frac{\partial\mathcal{L}}{\partial\hat{\mathbf{u}}_i}\mathcal{L}\left(\Omega,\mathbf{u}_1,\ldots,\mathbf{u}_N,\hat{\mathbf{w}}_1,\ldots,\hat{\mathbf{w}}_N\right)(\mathbf{u}_j'),\end{aligned}\tag{17}$$

where $\mathbf{u}_j'$ is the Eulerian derivative of $\mathbf{u}_j$, defined as the derivative of the mapping $t\mapsto\mathbf{u}_j(\Omega_{t\boldsymbol{\theta}})$ in $t=0$.

Next, we derive the equations for the adjoint states $\mathbf{w}_1,\ldots,\mathbf{w}_N$ solving the equations $\frac{\partial\mathcal{L}}{\partial\hat{\mathbf{u}}_j}=0$ for $j=1\ldots N$. For any $\mathbf{v}\in\mathrm{H}^1(\mathbb{R}^d)$ we have:

$$\begin{aligned}0&=\frac{\partial\mathcal{L}}{\partial\hat{\mathbf{u}}_j}(\Omega,\mathbf{u}_1,\ldots,\mathbf{u}_N,\mathbf{w}_1,\ldots,\mathbf{w}_N)(\mathbf{v})\\ &=\sum_{i=1}^{m}\sum_{\vec{\mathbf{k}}\in\mathcal{A}^{i,j}_{(1,m),N}}\alpha(\vec{\mathbf{k}})\left(\frac{\partial q_1}{\partial\hat{\mathbf{u}}_i}(\mathbf{u}_1,\ldots,\mathbf{u}_N)(\mathbf{v})+\frac{\partial q_2}{\partial\hat{\mathbf{U}}_i}(\mathbf{u}_1,\ldots,\mathbf{u}_N):(\nabla\mathbf{v})\right)\\ &-\int_\Omega\left(\boldsymbol{\sigma}\left(\mathbf{w}_j\right):\boldsymbol{\varepsilon}\left(\mathbf{v}\right)\right)\mathrm{d}\mathbf{x}+\int_{\Gamma_\mathrm{D}}\left(\mathbf{w}_j\cdot\left(\boldsymbol{\sigma}\left(\mathbf{v}\right)\mathbf{n}\right)+\mathbf{v}\cdot\left(\boldsymbol{\sigma}\left(\mathbf{w}_j\right)\mathbf{n}\right)\right)\mathrm{d}\mathbf{s}\\ &=\int_\Omega\left(\sum_{i=1}^{m}\sum_{\vec{\mathbf{k}}\in\mathcal{A}^{i,j}_{(1,m),N}}\alpha(\vec{\mathbf{k}})\left\{\frac{\partial q_1}{\partial\hat{\mathbf{u}}_i}-\left(\operatorname{div}\frac{\partial q_2}{\partial\hat{\mathbf{U}}_i}\right)\right\}+\operatorname{div}\mathbf{w}_j\right)\cdot\mathbf{v}\,\mathrm{d}\mathbf{x}\\ &+\int_{\Gamma_\mathrm{N}}\left(-\boldsymbol{\sigma}\left(\mathbf{w}_j\right)\mathbf{n}+\left(\frac{\partial q_2}{\partial\hat{\mathbf{U}}_i}\right)^T\mathbf{n}\right)\cdot\mathbf{v}\,\mathrm{d}\mathbf{s}+\int_{\Gamma_\mathrm{D}}\mathbf{w}_j\left(\boldsymbol{\sigma}\left(\mathbf{v}\right)\mathbf{n}\right)\mathrm{d}\mathbf{s}.\end{aligned}$$

The adjoint system eq. (14) can be retrieved from this result by choosing a generic $\mathbf{v}$ with compact support in Ω (for the differential equation), and by variating the trace of $\mathbf{v}$ on Γ_N and the normal stress $\boldsymbol{\sigma}(\mathbf{v})\mathbf{n}$ on Γ_D (for the boundary conditions).

By taking $\mathbf{w}_1,\ldots,\mathbf{w}_N$ as solutions of problem (14) for $j=1\ldots N$, we can further simplify the expression eq. (17) for the shape derivative of $\mathbb{E}\left[Q_m^\Omega(\mathbf{u}_\Omega,\cdots,\mathbf{u}_\Omega)\right]$ and obtain:

$$\begin{aligned}\frac{\mathrm{d}}{\mathrm{d}\Omega}\mathbb{E}\left[Q_m^\Omega(\mathbf{u}_\Omega,\cdots,\mathbf{u}_\Omega)\right](\boldsymbol{\theta}) &= \frac{\mathrm{d}}{\mathrm{d}\Omega}\mathcal{L}\left(\Omega,\mathbf{u}_1,\ldots,\mathbf{u}_N,\mathbf{w}_1,\ldots,\mathbf{w}_N\right)\\ &= \frac{\partial\mathcal{L}}{\partial\Omega}\left(\Omega,\mathbf{u}_1,\ldots,\mathbf{u}_N,\mathbf{w}_1,\ldots,\mathbf{w}_N\right)(\boldsymbol{\theta}).\end{aligned}\tag{18}$$

For simplicity, we consider the portions Γ_{N} and Γ_{D} of the boundary to be non-optimizable, which is equivalent to narrow the set of admissible displacement fields $\boldsymbol{\theta}$ to the set Θ_{adm} defined as:

$$\Theta_{adm} = \left\{ \boldsymbol{\theta} \in \mathrm{W}^{1,\infty}\left(\mathbb{R}^d, \mathbb{R}^d\right) \,:\, \boldsymbol{\theta} = 0 \text{ on } \Gamma_{\mathrm{D}} \cup \Gamma_{\mathrm{N}} \right\}.$$

Thanks to the restriction of the admissible displacement fields to Θ_{adm} and to Theorem 5.2.2 of [5] about the differentiation of integral functionals on variable domains, we conclude that the shape derivative of $\mathbb{E}\left[Q_m^{\Omega}(\mathbf{u}_\Omega, \cdots, \mathbf{u}_\Omega)\right]$ can be expressed as follows:

$$\begin{aligned}
\frac{\mathrm{d}}{\mathrm{d}\Omega}\mathbb{E}\left[Q_m^{\Omega}(\mathbf{u}_\Omega, \cdots, \mathbf{u}_\Omega)\right](\boldsymbol{\theta}) &= \frac{\mathrm{d}}{\mathrm{d}\Omega}\mathcal{L}\left(\Omega, \mathbf{u}_1, \ldots, \mathbf{u}_N, \mathbf{w}_1, \ldots, \mathbf{w}_N\right) \\
&= \frac{\partial \mathcal{L}}{\partial \Omega}\left(\Omega, \mathbf{u}_1, \ldots, \mathbf{u}_N, \mathbf{w}_1, \ldots, \mathbf{w}_N\right)(\boldsymbol{\theta}) \\
&= \sum_{\vec{\mathbf{k}} \in \mathcal{A}_{(1,m),N}} \left(\alpha(\vec{\mathbf{k}}) \int_{\Gamma_0} (\boldsymbol{\theta}\cdot\mathbf{n})\, q_1(\mathbf{u}_{k1}, \ldots, \mathbf{u}_{km})\, \mathrm{d}\mathbf{s} \right. \\
&\qquad \left. + \int_{\Gamma_0} (\boldsymbol{\theta}\cdot\mathbf{n})\, q_2(\nabla\mathbf{u}_{k1}, \ldots, \nabla\mathbf{u}_{km})\, \mathrm{d}\mathbf{s} \right) \\
&\qquad - \sum_{i=1}^{m} \int_{\Gamma_0} (\boldsymbol{\theta}\cdot\mathbf{n})\left(\boldsymbol{\sigma}\left(\mathbf{u}_i\right) : \boldsymbol{\varepsilon}\left(\mathbf{w}_i\right)\right)\, \mathrm{d}\mathbf{s}.
\end{aligned}$$

4 Application: structural optimization under constraints on the von Mises stress

4.1 Estimate of the expected value of the von Mises stress

An interesting application of polynomial functionals in shape optimization is related to the approximation of the $L-\infty$ norm of a given quantity in a structure by the L^m-norm, for m sufficiently big. A significant concern in structural mechanics is the design of structures where the stress is as evenly distributed as possible, preventing stress concentrations that could compromise the integrity of the component. This requirement suggests the use of functionals with order $m > 2$ for industrial applications, in order to better penalize stress concentrations with respect to quadratic functionals.

In the following section, we study the optimization of a 3D linear elastic structure with respect to its volume and the L^m-norm of the von Mises stress, for $m \geq 2$ even integer. We suppose that the optimization problem is framed as eq. (10), and that the random external load $\mathbf{g} \in \mathrm{L}^m\left(\mathcal{O}, \mathbb{P};\, \mathrm{L}^2(\Omega)\right)$ can be decomposed as in eq. (4).

We introduce the von Mises stress as reported in Section 4.5.6 of [29] and in [2].

Definition 4.1 (Deviatoric tensors and von Mises stress) *In each point of the domain $\Omega \subset \mathbb{R}^3$, we define the **deviatoric components** of the strain and stress tensors as follows:*

$$\boldsymbol{\varepsilon}_D(\mathbf{u}) = \boldsymbol{\varepsilon}(\mathbf{u}) - \frac{1}{d}\mathbb{I}\,\mathrm{tr}\,\boldsymbol{\varepsilon}(\mathbf{u}) = \boldsymbol{\varepsilon}(\mathbf{u}) - \frac{1}{d}\mathbb{I}\,\mathrm{div}\,\mathbf{u}$$
$$\boldsymbol{\sigma}_D(\mathbf{u}) = \boldsymbol{\sigma}(\mathbf{u}) - \frac{1}{d}\mathbb{I}\,\mathrm{tr}\,\boldsymbol{\sigma}(\mathbf{u}) = 2\mu\,\boldsymbol{\varepsilon}(\mathbf{u}) - \frac{2\mu}{d}\,\mathrm{tr}\,\boldsymbol{\varepsilon}(\mathbf{u}) = 2\mu\,\boldsymbol{\varepsilon}_D(\mathbf{u}).$$

*The **von Mises** stress is defined in each point of the domain as:*

$$s_D(\mathbf{u}) = \sqrt{\frac{d}{2}\,(\boldsymbol{\sigma}_D(\mathbf{u}) : \boldsymbol{\sigma}_D(\mathbf{u}))}.$$

We are interested in estimating the expected value of the functional

$$\Omega \mapsto \mathcal{G}_m(\Omega, \mathbf{g}) = G_m(\mathbf{u}, \dots, \mathbf{u}), \tag{19}$$

where $G_m : \mathrm{W}^{1,m}\left(\Omega, \mathbb{R}^3\right) \to \mathbb{R}$ is such that

$$G_m(\mathbf{v}_1, \dots, \mathbf{v}_m) = \int_\Omega \left((\boldsymbol{\sigma}_D(\mathbf{v}_1) : \boldsymbol{\sigma}_D(\mathbf{v}_2)) \dots ((\boldsymbol{\sigma}_D(\mathbf{v}_{m-1}) : \boldsymbol{\sigma}_D(\mathbf{v}_m))\right) \mathrm{d}\mathbf{x}. \tag{20}$$

At first, we can observe that, for a given displacement field $\mathbf{u} \in \mathrm{H}^1(\Omega) \cap \mathrm{W}^{1,m}(\Omega)$, the quantity $G_m(\mathbf{u}, \dots, \mathbf{u})$ is equal to the L^m-norm of the von Mises stress $s_D(\mathbf{u})$ in Ω, elevated to the power m:

$$G_m(\mathbf{u}, \dots, \mathbf{u}) = \left(\int_\Omega |s_D(\mathbf{u})|^m \,\mathrm{d}\mathbf{x}\right) = \|s_D(\mathbf{u})\|^m_{\mathrm{L}^m(\Omega)}.$$

Moreover, because of the concavity of the mapping $x \mapsto \sqrt[m]{x}$, the following bound on the expectation of the L^m-norm of the von Mises stress holds:

$$\mathbb{E}\left[\|s_D(\mathbf{u})\|_{\mathrm{L}^m(\Omega)}\right] \leq \left(\mathbb{E}\left[G_m(\mathbf{u}, \dots, \mathbf{u})\right]\right)^{\frac{1}{m}}. \tag{21}$$

Finally, we remark that the functional G_m respects the structure defined in eq. (12). Therefore, we can apply proposition 3.3 to compute the shape derivative of the functional $\Omega \mapsto \mathcal{G}_m(\Omega, \mathbf{g})$. The expression of the functional can be further simplified by considering the symmetries between the arguments of $\mathcal{G}_m$. Indeed, let us establish the following notation.

Definition 4.2 • *We denote*

$$\mathcal{B}_{\ell,N} = \left\{ \vec{\boldsymbol{\rho}} \in \mathbb{N}^{N\times N} : 1 \leq \rho_{ij} \leq \ell \;\; \textit{and} \;\; \sum_{i,j=1}^{N} \rho_{ij} = \ell \right\}$$

the set of all $N \times N$ integer matrices whose entries are positive and their sum is equal to ℓ. The cardinality of such set can be computed as $|\mathcal{B}_{\ell,N}| = \binom{N^2+\ell-1}{\ell}$.

- *For ℓ and N positive integers and $\vec{\boldsymbol{\rho}} \in \mathcal{B}_{\ell,N}$, we define the following* ***multinomial coefficient***

$$\binom{\ell}{\vec{\boldsymbol{\rho}}} = \frac{\ell!}{\prod_{i,j=1}^{N}(\rho_{i,j}!)}.$$

- *For N real random variables $\xi_1, \dots, \xi_m \in \mathrm{L}^m(\mathcal{O}, \mathbb{P}; \mathbb{R})$ and $\vec{\boldsymbol{\rho}} \in \mathcal{B}_{\frac{m}{2},N}$, we denote:*

$$K(\vec{\boldsymbol{\rho}}) = \binom{\frac{m}{2}}{\vec{\boldsymbol{\rho}}} \prod_{j=1}^{N} \mu_{\sum_{k=1}^{N}(\rho_{kj}+\rho_{jk}),j}.$$

Having introduced the necessary notation to take into account the symmetries among the arguments, we can write the expectation of the functional $\mathcal{G}_m(\Omega, \mathbf{g})$ as follows:

$$\mathbb{E}\left[\mathcal{G}_m(\Omega, \mathbf{g})\right] = \sum_{\vec{\boldsymbol{\rho}} \in \mathcal{B}_{\frac{m}{2},N}} \left\{ K(\vec{\boldsymbol{\rho}}) \int_{\Omega} \prod_{j,k=1}^{N} \left(\boldsymbol{\sigma}_D(\mathbf{u}_j) : \boldsymbol{\sigma}_D(\mathbf{u}_k)\right)^{\rho_{jk}} \mathrm{d}\mathbf{x} \right\}, \tag{22}$$

where each $\mathbf{u}_j$ solves the state equation eq. (11) with the external loading $\mathbf{g}_j$ for $j = 1 \dots N$.

Since the functional G_m respects the structure defined in eq. (12), we can apply proposition 3.3 and find the following expression for the shape derivative of $\mathbb{E}\left[\mathcal{G}_m(\Omega, \mathbf{g})\right]$:

$$\begin{aligned} \frac{\mathrm{d}}{\mathrm{d}\Omega}\mathbb{E}\left[\mathcal{G}_m(\Omega, \mathbf{g})\right](\boldsymbol{\theta}) = \int_{\Gamma_0} (\boldsymbol{\theta} \cdot \mathbf{n}) \Bigg(& -\sum_{j=1}^{N} \left(\boldsymbol{\sigma}\left(\mathbf{u}_j\right) : \boldsymbol{\varepsilon}\left(\mathbf{w}_j\right)\right) \\ & + \sum_{\vec{\boldsymbol{\rho}} \in \mathcal{B}_{\frac{m}{2},N}} \left\{ K(\vec{\boldsymbol{\rho}}) \prod_{j,k=1}^{N} \left(\boldsymbol{\sigma}_D(\mathbf{u}_j) : \boldsymbol{\sigma}_D(\mathbf{u}_k)\right)^{\rho_{jk}} \right\} \Bigg) \mathrm{d}\mathbf{s}. \end{aligned} \tag{23}$$

The adjoint states $\mathbf{w}_1, \dots, \mathbf{w}_N$ solve the following adjoint equations:

$$\begin{cases} -\operatorname{div}\boldsymbol{\sigma}\left(\mathbf{w}_j\right) = -2\mu \operatorname{div}\left(\sum_{k=1}^{N} L_{jk}\boldsymbol{\sigma}_D(\mathbf{u}_k)\right) & \text{in } \Omega \\ \boldsymbol{\sigma}\left(\mathbf{w}_j\right)\mathbf{n} = 2\mu \left(\sum_{k=1}^{N} L_{jk}\boldsymbol{\sigma}_D(\mathbf{u}_k)\right)\mathbf{n} & \text{on } \Gamma_0 \cup \Gamma_{\mathrm{N}} \\ \mathbf{w}_j = \mathbf{0} & \text{on } \Gamma_{\mathrm{D}}, \end{cases} \tag{24}$$

where the terms $L_{jk} \in \mathrm{L}^{m-1}(\Omega)$ are defined as:

$$L_{jk} = 2 \sum_{\vec{\boldsymbol{\rho}} \in \mathcal{B}_{\frac{m}{2},N}} \left(K(\vec{\boldsymbol{\rho}}) \rho_{jk} \left(\boldsymbol{\sigma}_D(\mathbf{u}_j) : \boldsymbol{\sigma}_D(\mathbf{u}_k) \right)^{\rho_{jk}-1} \prod_{\ell \neq k} \left(\boldsymbol{\sigma}_D(\mathbf{u}_j) : \boldsymbol{\sigma}_D(\mathbf{u}_\ell) \right)^{\rho_{j\ell}} \right).$$

We can notice also that, thanks to the symmetries of the von Mises functional G_m defined as in eq. (20), it is not necessary to compute all the $\left|\mathcal{B}_{\frac{m}{2},N}\right|$ terms of the sums in the formulae eq. (22) and eq. (23). Instead, the computation of $\mathcal{T}(G_m, N) = \binom{\frac{N(N+1)+m}{2}-1}{\frac{m}{2}}$ terms is sufficient, provided that they are counted with their respective multiplicity.

4.2 An optimization problem

In the following section, we study the following shape optimization problem:

$$\left|\begin{array}{l} \text{Find } \Omega_{opt} \in \mathcal{S}_{adm} \\ \text{minimizing } \Omega \mapsto \mathrm{Vol}(\Omega), \\ \text{where, for all } \omega \in \mathcal{O}, \text{ the state } \mathbf{u}_\Omega \in \left[\mathrm{H}^1(\Omega)\right]^d \text{ solves:} \\ \qquad \left\{\begin{array}{rcll} -\mathrm{div}\, \boldsymbol{\sigma}\left(\mathbf{u}_\Omega\right)(\omega) &=& \mathbf{0} & \text{in } \Omega, \\ \boldsymbol{\sigma}\left(\mathbf{u}_\Omega(\omega)\right)\mathbf{n} &=& \mathbf{g}(\Omega) & \text{on } \Gamma_{\mathrm{N}}, \\ \boldsymbol{\sigma}\left(\mathbf{u}_\Omega(\omega)\right)\mathbf{n} &=& \mathbf{0} & \text{on } \Gamma_0, \\ \mathbf{u}_\Omega(\omega) &=& \mathbf{0} & \text{on } \Gamma_{\mathrm{D}}. \end{array}\right. \\ \text{and the following constraint holds:} \\ \qquad \mathbb{E}\left[\mathcal{G}_6(\Omega, \mathbf{g})\right] \leq M_0^6, \end{array}\right. \tag{25}$$

where M_0 is a given upper bound for the constraint functional $\mathbb{E}\left[\mathcal{G}_6(\Omega, \mathbf{g})\right]$.

The structure to be optimized is a cylinder-like shape, centered on the axis $z = 0$, reported in fig. 1. Dirichlet boundary conditions are imposed on a thin stripe on the lateral surface, while the random load $\mathbf{g}$ is applied on a ring-shaped section on the upper surface of the structure. We consider the mechanical load $\mathbf{g} \in \mathrm{L}^6\left(\mathcal{O}, \mathbb{P};\ \mathrm{L}^6(\Gamma_{\mathrm{N}})\right)$ to have the following structure:

$$\mathbf{g}(\omega) = \mathbf{g}_1\, \xi_1(\omega) + \mathbf{g}_2\, \xi_2(\omega) \qquad \forall \omega \in \mathcal{O}.$$

The loads $\mathbf{g}_1$ and $\mathbf{g}_2$ are set as constant vectors on Γ_{N}, parallel to the axes x and y respectively, thus tangent to the surface. Moreover, we consider the random variables ξ_1 and ξ_2 to follow a centered gaussian distribution with variance σ_1 and σ_2 respectively.

From a numerical point of view, we represent the structure using a level-set function on a fixed mesh $\mathcal{T}_h$ covering a fixed domain D containing every admissible shape in $\mathcal{S}_{adm}$. The linear elasticity equations (11) and the adjoint problems (14) are defined on the entire domain $D = \Omega \cup \Omega^C$, using an *ersatz*

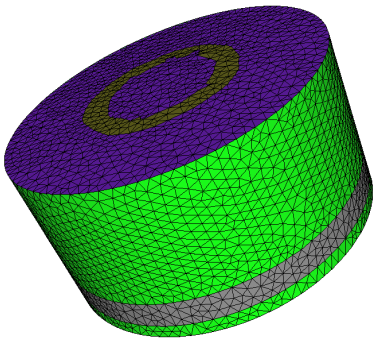

Fig. 1 Representation of the structure to be optimized. The surface Γ_{D} is the thin grey stripe on the lateral surface, while Γ_{N} is the ring-shaped portion of the upper surface marked in yellow.

material approximation in Ω^C to assure the well-posedness of the problems (see [7, 10]). The elasticity and adjoint equations are solved using the *FreeFem++* environment [31].

The optimization algorithm chosen to solve problem (25) is the *nullspace optimization* algorithm, introduced in [22]. Such algorithm requires the computation of the shape derivatives of the objective functional as well as of the constraints, motivating the application of the formula introduced in eq. (23) for the derivative of $\mathbb{E}\left[\mathcal{G}_6(\Omega, \mathbf{g})\right]$. The *nullspace optimization* algorithm is implemented in python. The packages *pyfreefem* (see [32, 33]) and *pymedit* (see [33, 34]) have been used to interface the python general framework with the *FreeFem++* finite-element solver and the methods for the computation of the signed-distance function [35] and advection of the level-set [36] provided in the ISCD toolbox [37].

The numerical results of two different simulations are discussed: in the first case we consider the random variables ξ_1 and ξ_2 to have an identical distribution (isotropic distribution of the external mechanical load), while the second caseconsiders an asymmetry in the variances of the two random variables (anisotropic distribution). The parameters used in the simulation are reported in table 1. The shapes obtained by the execution of 200 iterations of the *nullspace optimization* algorithm for both cases are reported in fig. 2, and the convergences of the objective and the constraint functions. All simulations have been performed on a Virtualbox virtual machine Linux with 1GB of dedicated memory, installed on a Dell PC equipped with a 2.80 GHz Intel i7 processor. The numerical results are reported in table 2.

From the observation of fig. 2 and fig. 3 we remark firstly the efficiency of the *nullspace optimization* algorithm in the solution of the constrained optimization problem (25). Indeed, the value of the objective functional decreases exponentially (see fig. 3a). As seen in fig. 3b, the constraint on the expectation of $\mathcal{G}_6$ is saturated in less than 50 iterations for the anisotropic case. In the isotropic case, we observe some oscillations in the constraint saturation

Heigth of the domain D	12.0	
Radius of the cylinder D	12.0	
Region Γ_{N}		
inner radius	4.0	
outer radius	6.0	
Region Γ_{D}		
thickness	2.0	
distance from the edge of D	1.0	
Mesh size parameters		
minimal element size `hmin`	0.4	
maximal element size `hmax`	0.8	
gradation value `hgrad`	1.3	
Elastic coefficients		
Young's modulus E	15	
Poisson's ration ν	0.35	
Ersatz material coefficient $\varepsilon_{\mathrm{ers}}$	10^{-3}	
Treshold M_0	3.0	
Variances of the random variables	isotropic	anisotropic
σ_1^2	2.5	1.0
σ_2^2	2.5	4.0
Number of iterations	200	

Table 1 Numerical parameters for problem (25) for the cases of random variables with equal and with different variances.

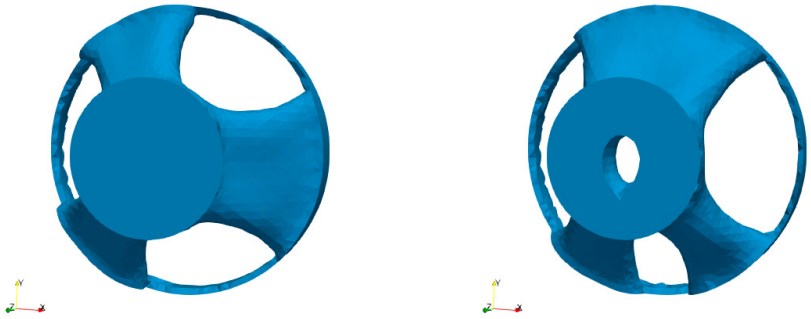

(a) Isotropic mechanical load (b) Anisotropic mechanical load

Fig. 2 Optimal shapes found by the nullspace optimization algorithm.

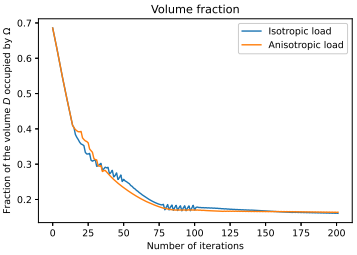

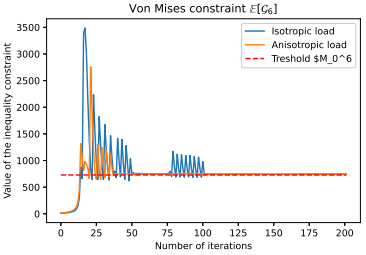

(a) Convergence of the volume of Ω, as the objective function.

(b) Convergence of the von Mises constraint $\mathbb{E}\left[\mathcal{G}_6(\Omega, \mathbf{g})\right] - M_0^6$.

Fig. 3 Convergence of the objective and constraint of problem (25)

	Isotropic case	Anisotropic case
Final volumic fraction $\mathrm{Vol}(\Omega_{opt})/\mathrm{Vol}(D)$	0.1608	0.164
Normalized saturation of the constraint $(\mathbb{E}[\mathcal{G}_6] - M_0^6)/M_0^6$	0.03002	0.005351
Execution time	129 minutes	148 minutes

Table 2 Numerical results of the solution of problem (25) for an isotropic and anisotropic mechanical load.

around iteration 80, which are due to a change in the topology around that step of the optimization. The shapes of fig. 2 show that a ramified structure presents the minimal volume ensuring enough resistence with respect to random mechanical loads. Moreover, if the direction of the mechanical load $\mathbf{g}(\cdot)$ is not uniformly distributed in the interval $[0, 2\pi]$, the branches tend to align parallel to the most probable direction of the load (see fig. 2b).

Finally, we remark that the constraint imposed in problem (25) is a quite conservative estimate for the expected value of the L^6-norm of the von Mises stress. Thanks to the inequality eq. (21) and the fact that the optimal shapes respect the constraint $\mathbb{E}[\mathcal{G}_6] \leq M_0^6$, we deduce that the average of the L^6-norm of the von Mises stress in the structures is actually less than the chosen treshold M_0.

5 Application: optimization of the variance of a quadratic functional

5.1 Expression of the variance of the mechanical compliance

The technique presented in section 3.2 can be applied to compute the shape derivative of the variance of a quadratic functional. As an example, we consider the optimization of a 2D bridge-like structure with respect to the expectation and the variance of the mechanical compliance. We recall that the compliance of a shape Ω is defined as the work of the external forces $\mathbf{g}$ acting on Ω (see e.g. [13]), and it can be expressed as:

$$\mathcal{C}(\Omega, \mathbf{g}) = C(\mathbf{u}_\Omega, \mathbf{u}_\Omega) = \int_\Omega \left(\boldsymbol{\sigma}\left(\mathbf{u}_\Omega\right) : \boldsymbol{\varepsilon}\left(\mathbf{u}_\Omega\right)\right) \mathrm{d}\mathbf{x},$$

where $\mathbf{u}_\Omega$ is the displacement computed as solution of the elasticity equation under the application of the load $\mathbf{g}$. From its expression, and from the fact that the elasticity equation is linear, we recognize that the compliance is a quadratic functional of the applied load $\mathbf{g}$.

We suppose that the structure Ω is enclosed in a square domain D of size 1.0×1.0, its lower side Γ_D is clamped, and a random uniform load $\mathbf{g}$ is applied on the upper side Γ_N (see fig. 5a). We consider the random load $\mathbf{g}$ to have the

following structure:

$$\mathbf{g}(\omega) = \mathbf{g}_0 + \xi(\omega)\,\mathbf{g}_x + \zeta(\omega)\,\mathbf{g}_y, \qquad \text{for all } \omega \in \mathcal{O}$$

where $\xi, \zeta \in \mathrm{L}^4(\mathcal{O}, \mathbb{P})$ are real random variables, and $\mathbf{g}_0 = (0, -g_0)$, $\mathbf{g}_x = (g_x, 0)$, and $\mathbf{g}_y = (0, -g_y)$. Under such hypotheses, the variance of the compliance can be written as:

$$\begin{aligned}
\mathrm{Var}\left[\mathcal{C}(\Omega, \mathbf{g})\right] &= \mathrm{Var}\left[C(\mathbf{u}_\Omega(\cdot), \mathbf{u}_\Omega(\cdot)\right] \\
&= \mathbb{E}\left[\xi^4\right] C(\mathbf{u}_x, \mathbf{u}_x)^2 + 4\mathbb{E}\left[\xi^3\,\zeta\right] C(\mathbf{u}_x, \mathbf{u}_x)\, C(\mathbf{u}_x, \mathbf{u}_y) \\
&\quad + \mathbb{E}\left[\xi^2\,\zeta^2\right] \left(2\, C(\mathbf{u}_x, \mathbf{u}_x)\, C(\mathbf{u}_y, \mathbf{u}_y) + 4\, C(\mathbf{u}_x, \mathbf{u}_y)^2\right) \\
&\quad + 4\mathbb{E}\left[\xi\,\zeta^3\right] C(\mathbf{u}_x, \mathbf{u}_y)\, C(\mathbf{u}_y, \mathbf{u}_y) + \mathbb{E}\left[\zeta^4\right] C(\mathbf{u}_y, \mathbf{u}_y)^2 \\
&\quad - \left(\mathbb{E}\left[\xi^2\right] C(\mathbf{u}_x, \mathbf{u}_x) + 2\,\mathbb{E}\left[\xi\,\zeta\right] C(\mathbf{u}_x, \mathbf{u}_y) + \mathbb{E}\left[\zeta^2\right] C(\mathbf{u}_y, \mathbf{u}_y)\right)^2 . \qquad (26)
\end{aligned}$$

Given $\beta, \alpha \in [0, \frac{\pi}{2})$, we define the following random variables:

$$\begin{aligned}
\xi_\alpha &= T \sin\alpha + N_\xi \cos\alpha, \\
\zeta_{\alpha,\beta} &= \frac{\sin\beta}{\sqrt{\mathrm{Var}\left[\xi_\alpha^2\right]}} \left(\xi_\alpha^2 - \mathbb{E}\left[\xi_\alpha^2\right]\right) + N_\zeta \cos\beta,
\end{aligned}$$

where $T \sim \mathcal{U}(\{-1, 1\})$, $N_\xi \sim \mathcal{N}(0, 1)$, and $N_\zeta \sim \mathcal{N}(0, 1)$ are independent random variables. The densities of the variables ξ_α and $\zeta_{\alpha,\beta}$ for different values of β and α are represented in fig. 4. It can be remarked that, unless $\beta = 0$, ξ_α and $\zeta_{\alpha,\beta}$ are not independent random variables. However, for any choice of $\beta, \alpha \in [0, \frac{\pi}{2})$, they are centered, normalized and uncorrelated, that is:

$$\mathbb{E}\left[\xi_\alpha\right] = \mathbb{E}\left[\zeta_{\alpha,\beta}\right] = 0, \qquad \mathbb{E}\left[\xi_\alpha^2\right] = \mathbb{E}\left[\zeta_{\alpha,\beta}^2\right] = 1, \qquad \mathbb{E}\left[\xi_\alpha\,\zeta_{\alpha,\beta}\right] = 0.$$

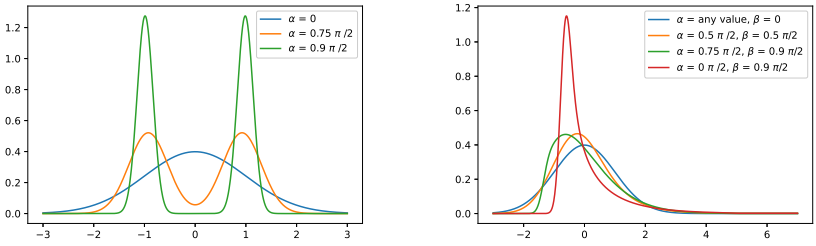

(a) Density of ξ_α (b) Density of $\zeta_{\alpha,\beta}$

Fig. 4 Densities of the variables ξ_α and $\zeta_{\alpha,\beta}$ for different values of β and α.

A deterministic expression for the variance of a generic cost functional has been proposed in [17] for the case of small perturbations, using a linearization procedure. However, eq. (26) provides a deterministic expression for the variance of the compliance without any assumption on the size of the uncertainties, and can be differentiated thanks to proposition 3.3.

5.2 An optimization problem for the variance of the compliance

Given the setting outlined in section 5.1, we consider the following optimization problem:

$$
\begin{aligned}
&\text{Find } \Omega_{opt} \in \mathcal{S}_{adm} \\
&\text{minimizing } \Omega \mapsto \mathrm{Vol}(\Omega), \\
&\text{where, for all } \omega \in \mathcal{O}, \text{ the state } \mathbf{u}_\Omega \in \left[\mathrm{H}^1(\Omega)\right]^d \text{ solves:} \\
&\qquad \begin{cases} -\mathrm{div}\,\boldsymbol{\sigma}\left(\mathbf{u}_\Omega\right) = 0 & \text{in } \Omega, \\ \boldsymbol{\sigma}\left(\mathbf{u}_\Omega(\omega)\right)\mathbf{n} = \mathbf{g}(\omega) & \text{on } \Gamma_{\mathrm{N}}, \\ \boldsymbol{\sigma}\left(\mathbf{u}_\Omega(\omega)\right)\mathbf{n} = 0 & \text{on } \Gamma_0, \\ \mathbf{u}_\Omega(\omega) = 0 & \text{on } \Gamma_{\mathrm{D}}. \end{cases} \\
&\text{and the following constraint holds:} \\
&\qquad \mathbb{E}\left[C(\mathbf{u}_\Omega(\omega), \mathbf{u}_\Omega(\omega))\right] \leq M_0, \\
&\qquad \mathrm{Var}\left[C(\mathbf{u}_\Omega(\omega), \mathbf{u}_\Omega(\omega))\right] \leq M_1.
\end{aligned}
\tag{27}
$$

The terms M_0 and M_1 are tresholds for the expectation and the variance of the compliance not to be exceeded.

At first, we remark that, without the constraint on the variance, the solution of eq. (27) would be the same for any choice of $\beta, \alpha \in [0, \frac{\pi}{2})$. Indeed, as stated in proposition 3.2 the value of $\mathbb{E}\left[C(\mathbf{u}_\Omega(\omega), \mathbf{u}_\Omega(\omega))\right]$ is a function of $\mathrm{Cor}_2(\mathbf{g}, \mathbf{g})$ which depends only on the first two moments of the variables ξ_α and $\zeta_{\alpha,\beta}$. Yet, ξ_α and $\zeta_{\alpha,\beta}$ share the same expected value, variance and correlation, for any $\beta, \alpha \in [0, \frac{\pi}{2})$.

The optimization is performed numerically using the *nullspace optimization* algorithm on an adaptive 2D mesh, as in [22] using the *mmg* platform for the mesh adaptation [38, 39]. The results of two simulations are presented, using different parameters α and β. In both cases, we used as initial condition the structure shown in fig. 5b. The numerical parameters are listed in table 3, and the results in table 4. Once again, the simulations have been done on a Dell PC with a 2.80 GHz Intel i7 processor, using a Virtualbox virtual machine Linux with 1GB of dedicated memory.

The evolution of the expectation and variance of the compliance, the evolution of the volume and the final results of the optimization in the two cases are represented in fig. 6, fig. 7, and fig. 8 respectively.

At first, we remark the similarity in the optimal structures for the two problems, represented in fig. 8. However, the structure in fig. 8a is thicker

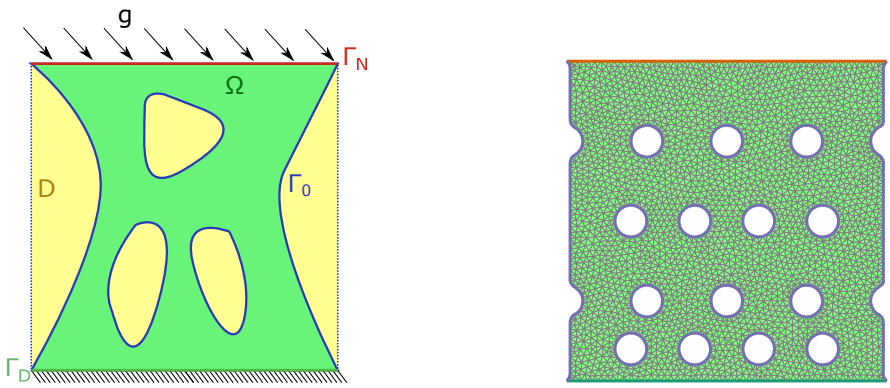

(a) Test case (b) Initial condition

Fig. 5 Representation of the test case described in section 5.1 and initial condition.

Heigth of the domain	1.0
Length of the domain	1.0
Mesh size parameters	
minimal element size `hmin`	0.01
maximal element size `hmax`	0.02
gradation value `hgrad`	0.5
Elastic coefficients	
Young's modulus E	15
Poisson's ration ν	0.35
Mechanical loads	
Fixed load $\mathbf{g}_0$	1.2
Horizontal term $\mathbf{g}_x$	1.0
Vertical term $\mathbf{g}_y$	0.3
Tresholds for the inequality constraints	
Treshold for the expected value M_0	2.0
Treshold for the variance M_0	3.0625
Number of iterations	500

Table 3 Numerical parameters for problem (26).

	Case 1	**Case 2**
Parameter α	0.0	$0.95\,\frac{\pi}{2}$
Parameter β	$0.95\,\frac{\pi}{2}$	0.0
Duration of the optimization	25.82 minutes	30.80 minutes
Final volume $\mathrm{Vol}(\Omega_{opt})$	0.435348	0.330348
Saturation of the constraints		
on the expected value $\mathbb{E}\left[C_{\Omega_{opt}}\right] - M_0$	-0.56886	0.004041
on the variance $\mathrm{Var}\left[C_{\Omega_{opt}}\right] - M_1$	0.03952	-2.94801

Table 4 Numerical results for the numerical solution of problem (26) for two sets of parameters α and β.

than fig. 8b, and the final volume of the solution of case 1 is 31% higher than the volume occupied by the solution of case 2. Such difference is explained by the fact that the variance of the compliance is significantly different in the two cases, as shown by fig. 6b. Indeed, in the first case, the constraint on the variance is saturated first, while in the second case the variance stays small throughout the optimization and the constraint on the expected value is saturated instead.

This example underlines the importance of the high order moments of the uncertainties in the domain of robust optimization, in particular when the random variables describing the boundary condition show a strong dependence from each other.

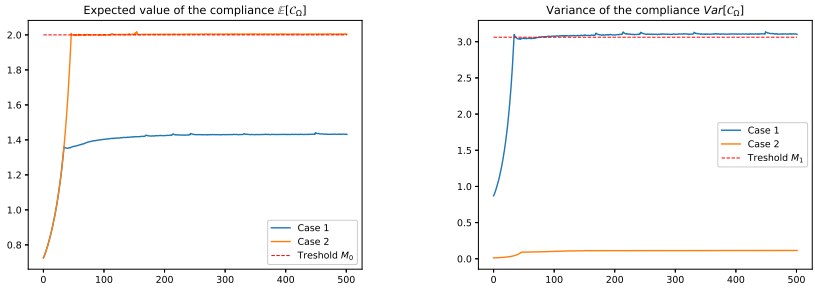

(a) Expectation of the compliance $\mathbb{E}[\mathcal{C}(\Omega, \mathbf{g})]$ (b) Variance of the compliance $\mathrm{Var}[\mathcal{C}(\Omega, \mathbf{g})]$

Fig. 6 Values of the expectation and the variance of the mechanical compliance throughout the optimization.

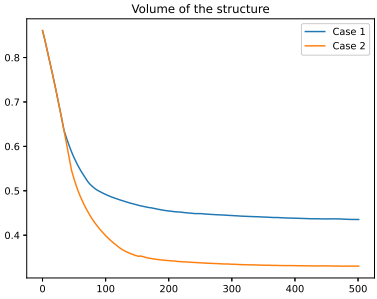

Fig. 7 Volume of the structure during the optimization problem for two choices of the parameters α and β.

6 Conclusions and perspectives

This article studied a procedure of shape optimization of polynomial functionals, where the external load applied to the structure is subject to uncertainties. Particular attention has been payed to the optimization of linear elastic structures, and we adopted the level-set approach to topology optimization. The present work proposed an extension of the technique proposed in [20] to the case of continuous multilinear functionals, and relies on the linearization properties of the tensor product between elements of a Banach space.

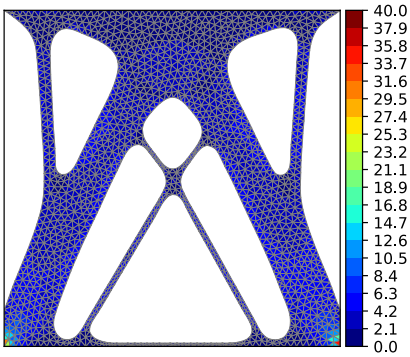

(a) Optimal structure for the choice of parameters $\alpha = 0.0$ and $\beta = 0.95\frac{\pi}{2}$ (case 1)

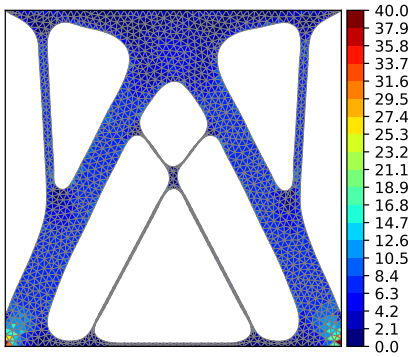

(b) Optimal structure for the choice of parameters $\alpha = 0.95\frac{\pi}{2}$ and $\beta = 0.0$ (case 2)

Fig. 8 Solution of the shape optimization problem (27) for two choices of α and β. The color scale represents the expectation of the concentration of the elastic energy $\boldsymbol{\sigma}(\mathbf{u}) : \boldsymbol{\varepsilon}(\mathbf{u})$.

After having introduced in section 2 the shape derivative according to Hadamard, the tensor product between multiple Banach spaces, and the Bochner spaces necessary to model the uncertainties, we presented the details of the method in section 3. In particular, we introduced the correlation tensor in order to express the expectation of the polynomial objective in terms of the first m moments of the random variables modeling the external loads (where m is the degree of the functional). Such tensor has been used it to compute a deterministic expression of the functional and its shape derivative. We presented two examples of numerical applications, highlighting the importance of shape optimization with respect to polynomial functionals in different contexts. Section 4 focused on the optimization of the mass of a tridimensional elastic structure, under a constraint on the expected value of the L^6-norm of the von Mises stress, aiming to avoid stress concentrations for a wide spectrum of external loads. As a second application, in section 5 we computed the derivative of the variance of the mechanical compliance in the case of a bidimensional structure, and we showed the importance of taking the variance into account when dealing with strongly correlated random variables.

A significant obstacle in the application of this method is the number of terms appearing in the sums of eq. (7) (for the computation of the functional of interest), and eq. (8) (for its derivative). Let us recall the definition of $\mathcal{T}(P_m, N)$ introduced at the end of section 3.2 as the minimal number of terms that are necessary to compute $\mathbb{E}[P_m(\mathbf{u}, \dots, \mathbf{u})]$ and its derivative, where P_m is a m-multilinear functional, and $\mathbf{u}$ is described by N random variables. Let us consider three different bounded m-multilinear functionals: a generic functional P_m, a functional S_m which is completely commutative in its arguments, and the von Mises functional G_m defined in eq. (20). We recall that in section 3.2 and in section 4.1 we found the following expressions for the number of terms

necessary to compute the expectations of such functionals:

$$\mathcal{T}(P_m, N) = N^m;$$
$$\mathcal{T}(S_m, N) = \binom{N+m-1}{m};$$
$$\mathcal{T}(G_m, N) = \binom{\frac{N(N+1)}{2} + \frac{m}{2} - 1}{\frac{m}{2}}.$$

As represented in fig. 9, the number of terms to be computed increases rapidly with the degree m of the multilinear functional, even if the number of random variables N is limited to 2 or 3. Naturally, the presence of symmetries in the multilinear mapping greatly reduces the number of terms to be computed, but the problem can still become too complex if the degree m required is sufficiently high.

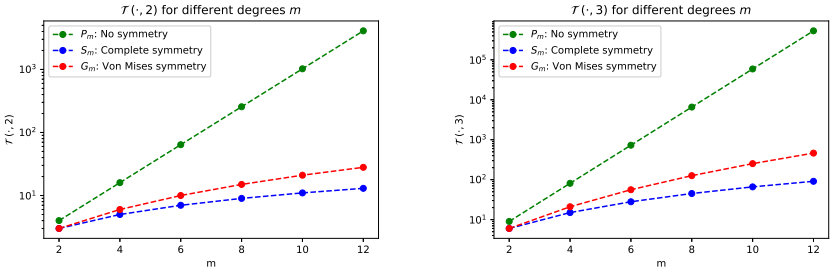

(a) Case of $N = 2$ random variables

(b) Case of $N = 3$ random variables

Fig. 9 Evaluation of $\mathcal{T}(P_m, N)$, $\mathcal{T}(S_m, N)$, and $\mathcal{T}(G_m, N)$ for different degrees m of the functionals examined.

As remedy to this issue, we suggest to exploit the symmetric nature of the correlation tensor, and study the application of some techniques of tensor decomposition. One promising solution consists in the approximation of the discretized correlation tensor as a sum of tensor of rank 1, using the CP-decomposition. Such technique and other kinds of tensor decompositions are detailed in [40], [41], and [42], and have been implemented in Python libraries as TensorLy [43]. However, its interpretation and applicability in the field of shape optimization are still to be investigated.

Appendix A Proofs

A.1 Proof of Proposition 2.2

In order to demonstrate that $\pi(\cdot)$ is a norm for the vector space $\bigotimes_{i=1}^{m} X_i$, we have to prove that the properties of absolute homogeneity, subadditivity, and positive definiteness hold.

1. **Absolute homogeneity.** Let us consider $\lambda \in \mathbb{R}$, and $u \in \bigotimes_{i=1}^{m} X_i$. By definition of product space, we can represent u as

$$u = \sum_{j=1}^{N} \bigotimes_{i=1}^{m} x_i^j$$

for N positive integer and some $x_i^j \in X_i$. Thanks to the definition 2.3, we know that

$$\pi(u) \leq \sum_{j=1}^{N} \prod_{i=1}^{m} \left\| x_i^j \right\|_{X_i}. \tag{A1}$$

The element (λu) of the product space can be represented as

$$\lambda u = \sum_{j=1}^{N} \bigotimes_{i=1}^{m} x_i^j.$$

Thanks to the inequality eq. (A1), we have that:

$$\pi(\lambda u) \leq \sum_{j=1}^{N} |\lambda| \left(\prod_{i=1}^{m} \left\| x_i^j \right\|_{X_i} \right) = |\lambda| \sum_{j=1}^{N} \left(\prod_{i=1}^{m} \left\| x_i^j \right\|_{X_i} \right).$$

Since such estimate holds for any representation of u, it follows that $\pi(\lambda u) \leq |\lambda| \pi(u)$. However, the reverse inequality is also true. Indeed:

$$|\lambda| \pi(u) = |\lambda| \pi\left(\lambda^{-1} \lambda u\right) \leq |\lambda| |\lambda^{-1}| \pi(\lambda u) = \pi(\lambda u).$$

Therefore $\pi(\lambda u) = |\lambda| \pi(u)$ for all real λ.

2. **Subadditivity.** Let us consider $u, v \in \bigotimes_{i=1}^{m} X_i$ and a real $\epsilon > 0$. Thanks to definition 2.3, there exist two positive integers N_u, N_v and two representations $u = \sum_{j=1}^{N_u} \bigotimes_{i=1}^{m} x_i^j$ and $v = \sum_{k=1}^{N_v} \bigotimes_{i=1}^{m} y_i^k$ such that

$$\sum_{j=1}^{N_u} \prod_{i=1}^{m} \left\| x_i^j \right\|_{X_i} \leq \pi(u) + \frac{\epsilon}{2}, \qquad \sum_{k=1}^{N_v} \prod_{i=1}^{m} \left\| y_i^k \right\|_{X_i} \leq \pi(v) + \frac{\epsilon}{2}.$$

Moreover, we have that $u + v = \sum_{j=1}^{N_u} \bigotimes_{i=1}^{m} x_i^j + \sum_{k=1}^{N_v} \bigotimes_{i=1}^{m} y_i^k$. By consequence, using the inequality eq. (A1), we have

$$\pi(u+v) \leq \sum_{j=1}^{N_u} \prod_{i=1}^{m} \left\| x_i^j \right\|_{X_i} + \sum_{k=1}^{N_v} \prod_{i=1}^{m} \left\| y_i^k \right\|_{X_i} \leq \pi(u) + \pi(v) + \epsilon.$$

Since such result holds for any $\epsilon > 0$, we can conclude that $\pi(u+v) \leq \pi(u) + \pi(v)$.

3. **Positive definiteness.** It is evident that $\pi(u)$ is a non-negative function. What needs to be proven is that $\pi(u) = 0$ implies $u = 0$. Let $u \in \bigotimes_{i=1}^{m} X_i$ be such that $\pi(u) = 0$, and we chose a representation $u = \sum_{j=1}^{N} \bigotimes_{i=1}^{m} x_i^j$ such that $\sum_{j=1}^{N} \prod_{i=1}^{m} \left\| x_i^j \right\|_{X_i} < \epsilon$. We denote by X_i^* the topological dual of the normed vector space X_i. We consider m bounded linear operators $\phi_i \in X_i$ for all $i = 1 \dots m$, and let $Q_m \in \hat{\mathfrak{P}}_m(X_1, \dots, X_m)$ be a multilinear operator such that $Q_m(\bigotimes_{i=1}^{m} y_i) = \prod_{i=1}^{m} \phi_i(y_i)$. Using the continuity of the operators ϕ_i and the choice of the representation of u, we get:

$$
\begin{aligned}
|Q_m(u)| = \left| \sum_{j=1}^{N} \prod_{i=1}^{m} \phi_i(x_i^j) \right| &\leq \sum_{j=1}^{N} \prod_{i=1}^{m} \|\phi_i\|_{X_i^*} \left\| x_i^j \right\|_{X_i} \\
&= \left(\prod_{i=1}^{m} \|\phi_i\|_{X_i^*} \right) \sum_{j=1}^{N} \prod_{i=1}^{m} \left\| x_i^j \right\|_{X_i} \leq \epsilon \left(\prod_{i=1}^{m} \|\phi_i\|_{X_i^*} \right).
\end{aligned}
$$

Since such estimate is independent from the representation and holds for all $\epsilon > 0$, we deduce that $|Q_m(u)| = 0$, meaning that, for any choice of the operators $\phi_i \in X_i^*$,

$$
\left| \sum_{j=1}^{N} \prod_{i=1}^{m} \phi_i(x_i^j) \right| = 0. \tag{A2}
$$

Let $A \in \hat{\mathfrak{P}}_m(X_1, \dots, X_m)$ be a multilinear functional. Thanks to the representation of u and to definition 2.2, $u(A) = \sum_{j=1}^{N} A(x^j{}_1, \dots, x^j{}_m)$. Let us define, for all $i = 1 \dots m$, $Y_i = \operatorname{span}\left\{ x_i^1, \dots, x_i^N \right\}$. Each Y_i is a subspace of X_i with finite dimension less than N. We define the multilinear functional $B \in \hat{\mathfrak{P}}_m(Y_1, \dots, Y_m)$ that coincides with A on its domain of definition. Since all Y_i are finite dimensional vector spaces, we can decompose the multilinear functional as follows:

$$
B(y_1, \dots, y_m) = \sum_{k=1}^{M} \prod_{i=1}^{m} \widehat{\psi_i^k}(y_i),
$$

where M is a positive integer and, for all $k = 1 \dots M$, $i = 1 \dots m$, $\widehat{\psi_i^k} \in Y_i^*$ (all functional $\widehat{\psi_i^k}$ is continuous because its domain is finite-dimensional). Thus, for each $\widehat{\psi_i^k}$, we can find an extension $\psi_i^k \in X_i^*$ thanks to Hahn-Banach's extension theorem (see Theorem 1.6.1 of [24]). Therefore,

considering the result eq. (A2), we can state that:

$$|u(A)| = \left|\sum_{j=1}^{N} A(x^j{}_1, \ldots, x^j{}_m)\right| = \left|\sum_{j=1}^{N} B(x^j{}_1, \ldots, x^j{}_m)\right|$$
$$= \left|\sum_{j=1}^{N}\sum_{k=1}^{M}\prod_{i=1}^{m}\psi_i^k(x_i^j)\right| \leq \sum_{k=1}^{M}\left|\sum_{j=1}^{N}\prod_{i=1}^{m}\psi_i^k(x_i^j)\right| = 0.$$

Having proved that $\pi(\cdot)$ is a norm for the vector space $\bigotimes_{i=1}^{m} X_i$, we have to show that $\pi\left(\bigotimes_{i=1}^{m} x_i\right) = \prod_{i=1}^{m} \|x_i\|_{X_i}$. At first, it follows directly from definition 2.3 that

$$\pi\left(\bigotimes_{i=1}^{m} x_i\right) \leq \prod_{i=1}^{m} \|x_i\|_{X_i}.$$

In order to prove the reverse inequality, we consider the linear operators $\phi_{x_i} \in X_i^*$ such that, for all $i = 1 \ldots m$, $\phi_{x_i}(x_i) = \|x_i\|_{X_i}$. We consider the multilinear operator $B \in \hat{\mathfrak{P}}_m(X_1, \ldots, X_m)$ mapping $(y_1, \ldots, y_m) \mapsto \prod_{i=1}^{m} \phi_{x_i}(y_i)$. Let $\widetilde{B} \in \left(\bigotimes_{i=1}^{m} X_i\right)'$ be the linearization of B, associating to any $u \in \bigotimes_{i=1}^{m} X_i$ the value $u(B)$. Let $u \in \bigotimes_{i=1}^{m} X_i$, represented as $u = \sum_{j=1}^{N} \bigotimes_{i=1}^{m} x_i^j$ for some $N > 0$. Then, we observe that

$$\left|\widetilde{B}(u)\right| = \left|\sum_{j=1}^{N} \widetilde{B}\left(\bigotimes_{i=1}^{m} x_i^j\right)\right| \leq \sum_{j=1}^{N}\left|\widetilde{B}\left(\bigotimes_{i=1}^{m} x_i^j\right)\right|$$
$$= \sum_{j=1}^{N}\left|\prod_{i=1}^{m}\phi_{x_i}(x_i)\right| \leq \sum_{j=1}^{N}\prod_{i=1}^{m}\left\|x_i^j\right\|_{X_i}.$$

Since such estimate is valid for any representation of u, we deduce that $\left|\widetilde{B}(u)\right| \leq \pi(u)$ for all $u \in \bigotimes_{i=1}^{m} X_i$. We have proved that, in the topology induced by the norm $\pi(\cdot)$, $\widetilde{B}$ is a continuous operator, and $\left\|\widetilde{B}\right\|_{OP} \leq 1$. Therefore, we deduce the following inequality:

$$\prod_{i=1}^{m} \|x_i\|_{X_i} = \widetilde{B}\left(\bigotimes_{i=1}^{m} x_i\right) \leq \pi\left(\bigotimes_{i=1}^{m} x_i\right).$$

However, the reverse inequality can be deduced directly from the definition 2.3 of the projective norm. Thus, we can conclude that

$$\prod_{i=1}^{m} \|x_i\|_{X_i} = \pi\left(\bigotimes_{i=1}^{m} x_i\right).$$

A.2 Proof of Proposition 2.3

Let us consider the real valued functional $\widetilde{P_m} : \bigotimes_{i=1}^m X_i \to \mathbb{R}$ such that, for any choice of $\{x_i^1 \dots x_i^N\} \subset X_i$,

$$\widetilde{P_m}\left(\sum_{j=1}^n \bigotimes_{i=1}^m x_i^j\right) = \sum_{j=1}^n P_m(x_1^j, \dots, x_m^j).$$

Thanks to definition 2.2, the functional $\widetilde{P_m}$ is well-defined on $\bigotimes_{i=1}^m X_i$.

The operator , $\widetilde{P_m}$ is bounded thanks to definition 2.3 of the projective norm and the continuity of the operator $P_m \in \mathfrak{P}_m(X_1, \dots, X_m)$. Indeed, let $u \in \bigotimes_{i=1}^m X_i$ be such that $\pi(u) = 1$, and let $\sum_{j=1}^N \bigotimes_{i=1}^m x_i^j$ a decomposition of u. Then, we have

$$\begin{aligned}\left|\widetilde{P_m}(u)\right| &= \left|\sum_{j=1}^N \widetilde{P_m}\left(\bigotimes_{i=1}^m x_i^j\right)\right| \\ &\leq \sum_{j=1}^N \left|P_m\left(x_1^j, \dots, x_m^j\right)\right| \leq \|P_m\|_{OP} \sum_{j=1}^N \prod_{i=1}^m \left\|x_i^j\right\|_{X_i}.\end{aligned}$$

By taking the infimum on the decompositions of u and the supremum on operators in $\bigotimes_{i=1}^m X_i$ with norm equal to 1, we get:

$$\left|\widetilde{P_m}(u)\right| \leq \|P_m\|_{OP} \inf_{u=\sum_{j=1}^N \bigotimes_{i=1}^m x_i^j} \sum_{j=1}^N \prod_{i=1}^m \left\|x_i^j\right\|_{X_i} = \|P_m\|_{OP};$$

which implies:

$$\left\|\widetilde{P_m}\right\|_{OP} = \sup_{\pi(u)=1} \left|\widetilde{P_m}(u)\right| \leq \|P_m\|_{OP}. \tag{A3}$$

In order to show that the norms of the operators $\widetilde{P_m}$ and P_m are equal, we prove the reverse inequality. Let $y_1, \dots, y_m$ be such that, for all $i = 1 \dots m$, $y_i \in X_i$ and $\|y_i\|_{X_i} = 1$. Therefore:

$$\begin{aligned}|P_m(y_1, \dots, y_m)| &= \left|\widetilde{P_m}\left(\bigotimes_{i=1}^m y_i\right)\right| \leq \left\|\widetilde{P_m}\right\|_{OP} \pi\left(\bigotimes_{i=1}^m y_i\right) \\ &= \left\|\widetilde{P_m}\right\|_{OP} \prod_{i=1}^m \|y_i\|_{X_i} = \left\|\widetilde{P_m}\right\|_{OP},\end{aligned}$$

which entails:

$$\|P_m\|_{OP} = \sup_{\|y_i\|_{X_i}=1} \left|\widetilde{P_m}(u)\right| \leq \left\|\widetilde{P_m}\right\|_{OP}. \tag{A4}$$

Thanks to the inequalities eq. (A3) and eq. (A4), we conclude that $\left\|\widetilde{P_m}\right\|_{OP} = \|P_m\|_{OP}$.

We have showed that $\widetilde{P_m}$ is a well-defined, bounded, linear operator defined on $\bigotimes_{i=1}^{m} X_i$, whose norm is equal to $\|P_m\|_{OP}$. Since $\bigotimes_{i=1}^{m} X_i$ is a subspace of $\widehat{\bigotimes}_{\pi,i=1}^{m} X_i$, we can apply the Hahn-Banach extension theorem (see *Theorem 1.6.1* of [24]) and conclude that there exists a bounded linear operator $\widehat{P_m}$ extending $\widetilde{P_m}$ on $\widehat{\bigotimes}_{\pi,i=1}^{m} X_i$ and such that $\left\|\widehat{P_m}\right\|_{OP} = \left\|\widetilde{P_m}\right\|_{OP} = \|P_m\|_{OP}$. Moreover, since $\bigotimes_{i=1}^{m} X_i$ is dense in $\widehat{\bigotimes}_{\pi,i=1}^{m} X_i$, the extension is unique.

References

[1] Allaire, G., Jouve, F.: Minimum stress optimal design with the level set method. Engineering Analysis with Boundary Elements **32**(11), 909–918 (2008). https://doi.org/10.1016/j.enganabound.2007.05.007.

[2] Amstutz, S., Novotny, A.A.: Topological optimization of structures subject to Von Mises stress constraints. Structural and Multidisciplinary Optimization **41**(3), 407–420 (2010). https://doi.org/10.1007/s00158-009-0425-x. Accessed 2022-01-19

[3] Simon, J., Murat, F.: Sur le contrôle par un domaine géométrique. Laboratoire d'Analyse Numérique de l'Université de Paris VI (1976)

[4] Allaire, G.: Conception Optimale de Structures. Mathématiques & applications, vol. 58. Springer, Berlin (2007). http://link.springer.com/10.1007/978-3-540-36856-4

[5] Henrot, A., Pierre, M.: Shape Variation and Optimization: a Geometrical Analysis. Tracts in Mathematics, vol. 28. European Mathematical Society, Zurich (2018).

[6] van Dijk, N.P., Maute, K., Langelaar, M., van Keulen, F.: Level-set methods for structural topology optimization: a review. Structural and Multidisciplinary Optimization **48**(3), 437–472 (2013). https://doi.org/10.1007/s00158-013-0912-y. Accessed 2023-01-06

[7] Allaire, G., Jouve, F., Toader, A.-M.: Structural optimization using sensitivity analysis and a level-set method. Journal of Computational Physics **194**(1), 363–393 (2004). https://doi.org/10.1016/j.jcp.2003.09.032. Accessed 2022-10-19

[8] Allaire, G., Dapogny, C., Frey, P.: Shape optimization with a level set based mesh evolution method. Computer Methods in Applied Mechanics and Engineering **282**, 22–53 (2014). https://doi.org/10.1016/j.cma.2014.08.028. Accessed 2022-01-31

[9] de Gournay, F.: Velocity Extension for the Level-set Method and Multiple Eigenvalues in Shape Optimization. SIAM Journal on Control and Optimization **45**(1), 343–367 (2006). https://doi.org/10.1137/050624108. Publisher: Society for Industrial and Applied Mathematics. Accessed 2022-03-02

[10] Dambrine, M., Kateb, D.: On the Ersatz material approximation in level-set methods. ESAIM: Control, Optimisation and Calculus of Variations **16**(3), 618–634 (2010). https://doi.org/10.1051/cocv/2009023. Accessed 2023-02-14

[11] Bendsøe, M.P.: Optimal shape design as a material distribution problem. Structural optimization **1**(4), 193–202 (1989). https://doi.org/10.1007/BF01650949. Accessed 2023-01-06

[12] Bendsøe, M., Sigmund, O.: Topology Optimization. Theory, Methods, and Applications. 2nd Ed., Corrected Printing, (2004). https://doi.org/10.1007/978-3-662-05086-6

[13] Allaire, G., Dapogny, C., Jouve, F.: Shape and Topology Optimization vol. 22. Elsevier, (2021). https://doi.org/10.1016/bs.hna.2020.10.004. https://linkinghub.elsevier.com/retrieve/pii/S1570865920300181

[14] Sigmund, O., Maute, K.: Topology optimization approaches. Structural and Multidisciplinary Optimization **48**(6), 1031–1055 (2013). https://doi.org/10.1007/s00158-013-0978-6. Accessed 2023-01-06

[15] Chen, S., Chen, W.: A new level-set based approach to shape and topology optimization under geometric uncertainty. Structural and Multidisciplinary Optimization **44**(1), 1–18 (2011). https://doi.org/10.1007/s00158-011-0660-9. Accessed 2023-01-06

[16] Dambrine, M., Harbrecht, H., Puig, B.: Computing quantities of interest for random domains with second order shape sensitivity analysis. ESAIM: Mathematical Modelling and Numerical Analysis **49**(5), 1285–1302 (2015). https://doi.org/10.1051/m2an/2015012. Number: 5 Publisher: EDP Sciences

[17] Allaire, G., Dapogny, C.: A deterministic approximation method in shape optimization under random uncertainties. SMAI Journal of Computational Mathematics **1**, 83–143 (2015). https://doi.org/10.5802/smai-jcm.5. Publisher: Société de Mathématiques Appliquées et Industrielles (SMAI)

[18] Chen, S., Chen, W., Lee, S.: Level set based robust shape and topology optimization under random field uncertainties. Structural and Multidisciplinary Optimization **41**(4), 507–524 (2010). https://doi.org/10.1007/

s00158-009-0449-2. Accessed 2023-01-06

[19] Dunning, P.D., Kim, H.A.: Robust Topology Optimization: Minimization of Expected and Variance of Compliance. AIAA Journal **51**(11), 2656–2664 (2013). https://doi.org/10.2514/1.J052183. Publisher: American Institute of Aeronautics and Astronautics _eprint: https://doi.org/10.2514/1.J052183. Accessed 2023-01-06

[20] Dambrine, M., Dapogny, C., Harbrecht, H.: Shape Optimization for Quadratic Functionals and States with Random Right-Hand Sides. SIAM Journal on Control and Optimization **53**(5), 3081–3103 (2015). https://doi.org/10.1137/15M1017041. Publisher: Society for Industrial and Applied Mathematics

[21] Allaire, G., Pantz, O.: Structural optimization with FreeFem++. Structural and Multidisciplinary Optimization **32**(3), 173–181 (2006). https://doi.org/10.1007/s00158-006-0017-y. Accessed 2022-10-10

[22] Feppon, F., Allaire, G., Dapogny, C.: Null space gradient flows for constrained optimization with applications to shape optimization. ESAIM: Control, Optimisation and Calculus of Variations **26**, 90 (2020). https://doi.org/10.1051/cocv/2020015. Publisher: EDP Sciences

[23] Ryan, R.A.: Introduction to Tensor Products of Banach Spaces. Springer Monographs in Mathematics. Springer, London (2002). https://doi.org/10.1007/978-1-4471-3903-4. http://link.springer.com/10.1007/978-1-4471-3903-4 Accessed 2022-08-23

[24] Kadison, R.V., Ringrose, J.R.: Elementary Theory: Fundamentals of the Theory of Operator Algebras vol. I. Elsevier, New York (1983)

[25] Hytönen, T., van Neerven, J., Veraar, M., Weis, L.: Analysis in Banach Spaces: Volume I: Martingales and Littlewood-Paley Theory. Ergebnisse der Mathematik und ihrer Grenzgebiete. 3. Folge. Springer, Cham (2016). https://doi.org/10.1007/978-3-319-48520-1

[26] Salsa, S.: Partial Differential Equations in Action: From Modeling To Theory, 3rd edn. UNITEXT. Springer, (2015)

[27] Martínez-Frutos, J., Esparza, F.P.: Optimal Control of PDEs Under Uncertainty: An Introduction with Application to Optimal Shape Design of Structures, 1st ed. 2018 édition edn. Springer, New York, NY (2018)

[28] Slaughter, W.S.: The Linearized Theory of Elasticity. Birkhäuser, Boston (2002).

[29] Jones, R.M.: Deformation Theory of Plasticity. Bull Ridge Corporation,

Blacksburg, Virginia (2008).

[30] Céa, J.: Conception optimale ou identification de formes, calcul rapide de la dérivée directionnelle de la fonction coût. ESAIM: Mathematical Modelling and Numerical Analysis - Modélisation Mathématique et Analyse Numérique **20**(3), 371–402 (1986). Accessed 2022-09-08

[31] Hecht, F.: New development in freefem++. Journal of Numerical Mathematics **20**(3-4), 1–14 (2012). https://doi.org/10.1515/jnum-2012-0013. Publisher: De Gruyter. Accessed 2022-11-02

[32] Feppon, F.: pyfreefem: Package PyFreeFEM for interfacing Python and FreeFEM. https://gitlab.com/florian.feppon/pyfreefem/ Accessed 2022-09-09

[33] Feppon, F.: Optimisation topologique de systèmes multiphysiques. PhD thesis, Université Paris Saclay (COmUE) (December 2019). https://tel.archives-ouvertes.fr/tel-02441844

[34] Feppon, F.: pymedit: Package pymedit for operating on 2D and 3D meshes in the INRIA mesh format. https://gitlab.com/florian.feppon/pymedit Accessed 2022-09-09

[35] Dapogny, C., Frey, P.: Computation of the signed distance function to a discrete contour on adapted triangulation. Calcolo **49**(3), 193–219 (2012). https://doi.org/10.1007/s10092-011-0051-z. Accessed 2022-03-17

[36] Dapogny, C., Dobrzynski, C., Frey, P.: Three-dimensional adaptive domain remeshing, implicit domain meshing, and applications to free and moving boundary problems. Journal of Computational Physics **262**, 358–378 (2014). https://doi.org/10.1016/j.jcp.2014.01.005. Accessed 2023-02-14

[37] Sorbonne, I.: ISCD toolbox. https://github.com/ISCDtoolbox

[38] Bui, C., Dapogny, C., Frey, P.: An accurate anisotropic adaptation method for solving the level set advection equation. International Journal for Numerical Methods in Fluids **70**(7), 899–922 (2012). https://doi.org/10.1002/fld.2730. _eprint: https://onlinelibrary.wiley.com/doi/pdf/10.1002/fld.2730. Accessed 2023-02-14

[39] Dapogny, C., Dobrzynski, C., Frey, P., Froehly, A.: Mmg Platform – Upgrade your meshes. http://www.mmgtools.org/ Accessed 2022-09-09

[40] Kolda, T.G., Bader, B.W.: Tensor Decompositions and Applications. SIAM Review **51**(3), 455–500 (2009). https://doi.org/10.1137/

07070111X. Accessed 2022-06-21

[41] Kolda, T.G.: Numerical optimization for symmetric tensor decomposition. Mathematical Programming **151**(1), 225–248 (2015). https://doi.org/10.1007/s10107-015-0895-0. Accessed 2022-12-02

[42] Comon, P., Luciani, X., de Almeida, A.L.F.: Tensor decompositions, alternating least squares and other tales. Journal of Chemometrics **23**(7-8), 393–405 (2009). https://doi.org/10.1002/cem.1236. _eprint: https://onlinelibrary.wiley.com/doi/pdf/10.1002/cem.1236. Accessed 2023-01-09

[43] Kossaifi, J., Panagakis, Y., Anandkumar, A., Pantic, M.: TensorLy: Tensor Learning in Python. Journal of Machine Learning Research **20**(26), 1–6 (2019). Accessed 2023-01-09